Fixation of Atmospheric CO_2 by a Series of Hydroxo Complexes of Divalent Metal Ions and the Implication for the Catalytic Role of Metal Ion in Carbonic Anhydrase. Synthesis, Characterization, and Molecular Structure of $[LM(OH)]_n$ (n = 1 or 2) and $LM(\mu\text{-}CO_3)ML$ (M(II) = Mn, Fe, Co, Ni, Cu, Zn; L = $HB(3,5\text{-}iPr_2pz)_3$)†

Nobumasa Kitajima,* Shiro Hikichi, Masako Tanaka, and Yoshihiko Moro-oka

Contribution from the Research Laboratory of Resources Utilization, Tokyo Institute of Technology, 4259 Nagatsuta, Midori-ku, Yokohama 227, Japan

Received May 12, 1992

Abstract: By using the hindered tris(pyrazolyl)borate ligand $HB(3,5\text{-}iPr_2pz)_3$, (hydrotris(3,5-diisopropyl-1-pyrazolyl)-borate), a series of hydroxo complexes of first-row divalent metal ions (Mn (**1**), Fe (**2**), Co (**3**), Ni (**4**), Cu (**5**), Zn (**6**)) was synthesized. X-ray crystallography was applied to **1–5**, establishing that all these hydroxo complexes have a dinuclear structure solely bridged with a bis(hydroxo) unit. The structure of **6** was characterized by spectroscopy, which indicates that **6** is monomeric. All these hydroxo complexes were found to react with CO_2, even atmospheric CO_2, to afford μ-carbonato dinuclear complexes of Mn (**7**), Fe (**8**), Co (**9**), Ni (**10**), Cu (**11**), and Zn (**12**). The molecular structures of the complexes **8–12** were determined. A variety of coordination modes of the carbonate group was seen. In **10** and **11**, the carbonate group is bound to both metal centers bidentately in a symmetric fashion, while in **8** and **9**, the carbonate coordination modes are described as an unsymmetric bidentate. The carbonate group in **12** is coordinated to one zinc ion bidentately, but it is bound to the other zinc ion unidentately. From IR data, the coordination mode of the carbonate group in **7** was suggested to be similar to those found in **8** and **9**. Thus, the order of the coordination distortions of the carbonate groups in this series of μ-carbonato dinuclear complexes is as follows: Zn > Mn ≈ Fe ≈ Co > Ni ≈ Cu. On the other hand, the reactivities of the hydroxo complexes toward CO_2 fixation were found to be ordered Zn > Cu > Ni ≈ Co > Mn > Fe. It is noteworthy that the order of the CO_2 fixation capabilities of the hydroxo complexes does not fit with the order of activities known for metal-substituted carbonic anhydrases. The order of activities for CO_2 hydration by the carbonic anhydrases is Zn > Co ≫ Ni ≈ Mn > Cu ≈ 0. Thus, the order is correlated mostly with the coordination distortions of the carbonate group in the μ-carbonate complexes but not the reactivities of the hydroxo complexes toward CO_2.

Introduction

A variety of insertion reactions of CO_2 into metal–ligand bonds is known.[1] In many systems, the insertion is initiated by a nucleophilic attack of the ligand anion to CO_2 (eq 1). When the

(1)

ligand anion is oxo or hydroxo, the reaction results in formation of a carbonato or bicarbonato complex. This type of reaction is known for Co,[2] Ni,[3] Cu,[4,5] and Zn[6] complexes. Churchill et al. reported the formation of μ-carbonato dinuclear copper(II) complexes upon the reaction of CuCl and a series of N-ligands such as amines under an O_2/CO_2 atmosphere.[4] The mechanistic exploration led to a conclusion that the initially formed intermediate is a μ-oxo dinuclear copper(II) complex, which subsequently reacts with CO_2 to give the product. As a proof for the suggestion, we have recently found that the isolated (μ-oxo)-[7] or bis(μ-hydroxo)copper(II) complex,[8] in fact, reacts readily with CO_2 to give μ-carbonato dinuclear copper(II) complexes.[5,9] In particular, the bis(μ-hydroxo) complex $[Cu(HB(3,5\text{-}iPr_2pz)_3)]_2(OH)_2$[8] exhibits remarkably high reactivity so as to react with atmospheric CO_2.[5]

The fixation of atmospheric CO_2 by hydroxo metal complexes is of special interest from the viewpoint of environmental protection, because the fundamental understanding and the application of the reaction may lead to some practical means to eliminate CO_2 present in air. The increase of atmospheric CO_2 causes serious environmental problems which should be overcome in the near future.[10] Thus, the development of an effective chemical method for CO_2 elimination is currently the focus of numerous investigations.[11]

† This paper is dedicated to Professor Richard H. Holm of Harvard University on the occasion of his 60th birthday.

(1) Palmer, D. A.; Van Eldik, R. *Chem. Rev.* **1983**, *83*, 651.
(2) Murase, I.; Vuckovic, G.; Kodera, M.; Harada, H.; Matsumoto, N.; Kida, S. *Inorg. Chem.* **1991**, *30*, 728.
(3) Tanase, T.; Nitta, S.; Yoshikawa, S.; Kobayashi, K.; Sakurai, T.; Yano, S. *Inorg. Chem.* **1992**, *31*, 1058.
(4) (a) Churchill, M. R.; Davies, G.; El-Sayed, M. A.; El-Shazly, M. F.; Hutchinson, J. P.; Rupich, M. W.; Watkins, K. O. *Inorg. Chem.* **1979**, *18*, 2296. (b) Churchill, M. R.; Davies, G.; El-Sayed, M. A.; El-Shazly, M. F.; Hutchinson, J. P.; Rupich, M. W. *Inorg. Chem.* **1980**, *19*, 201. A similar reaction was recently reported: Menif, R.; Reibenspies, J.; Martell, A. E. *Inorg. Chem.* **1991**, *30*, 3446.
(5) Kitajima, N.; Fujisawa, K.; Koda, T.; Hikichi, S.; Moro-oka, Y. *J. Chem. Soc., Chem. Commun.* **1990**, 1357.
(6) Alsfasser, R.; Trofimenko, S.; Looney, A.; Parkin, G.; Vahrenkamp, H. *Inorg. Chem.* **1991**, *30*, 4098.
(7) Kitajima, N.; Koda, T.; Moro-oka, Y. *Chem. Lett.* **1988**, 347.
(8) (a) Kitajima, N.; Fujisawa, K.; Moro-oka, Y. *Inorg. Chem.* **1990**, *29*, 357. (b) Kitajima, N.; Fujisawa, K.; Fujimoto, C.; Moro-oka, Y.; Hashimoto, S.; Kitagawa, T.; Toriumi, K.; Tatsumi, K.; Nakamura, A. *J. Am. Chem. Soc.* **1992**, *114*, 1277.
(9) Kitajima, N.; Koda, T.; Hashimoto, S.; Kitagawa, T.; Moro-oka, Y. *J. Am. Chem. Soc.* **1991**, *113*, 5664.
(10) See the recent papers and the references cited therein: (a) Marston, J. B.; Oppenheimer, M.; Fujita, R. M.; Gaffin, S. R. *Nature (London)* **1991**, *349*, 573. (b) Jenkinson, D. S.; Adams, D. E.; Wild, A. *Nature (London)* **1991**, *351*, 304.
(11) (a) Behr, A. *Chem.-Ing.-Tech.* **1985**, *57*, 893. (b) Behr, A. *Angew. Chem., Int. Ed. Engl.* **1988**, *27*, 661.

0002-7863/93/1515-5496$04.00/0

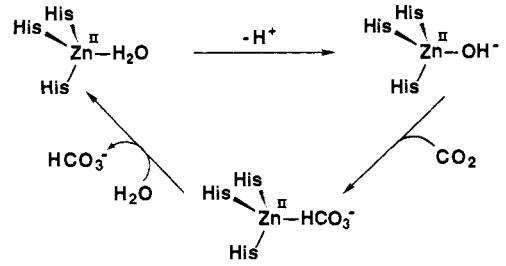

Figure 1. Proposed mechanism for CO_2 hydration by carbonic anhydrase via a hydroxide intermediate.

The nucleophilic fixation of CO_2 by hydroxo metal complexes to afford the metal bicarbonate or carbonate species is also relevant to the structures and functions of some metalloenzymes. D-Ribulose 1,5-bisphosphate carboxylase/oxygenase, designated Rubisco, the most abundant metalloenzyme on the earth, is a magnesium-containing protein that is responsible for fixation of CO_2 in the photosynthetic reaction operating in plants.[12] The trigger for initiating the catalysis is ascribed to the formation of a magnesium bicarbonate species, which may be formed via a magnesium hydroxide intermediate.[13] Other bicarbonate metal complexes playing an important role in biological systems include the non-heme iron in the photosynthetic system II[14] and transferrin;[15] in both systems, the coordination of a bicarbonate ion to the iron is suggested. The enzyme, whose function is apparently related directly to the fixation of CO_2 by hydroxo metal complexes, is carbonic anhydrase, which catalyzes the physiologically important hydration of CO_2 to bicarbonate as shown in eq 2.[16] The active site of carbonic anhydrase consists

$$CO_2 + H_2O \rightleftharpoons HCO_3^- + H^+ \quad (2)$$

of a monomeric zinc ion which is coordinated to three histidyl nitrogen atoms and a water.[17] In a generally accepted mechanism, deprotonation of the coordinated water generates a hydroxide ion on the zinc, which reacts with CO_2 as illustrated in Figure 1. While the zinc-containing carbonic anhydrase is the most effective, the zinc ion in carbonic anhydrase is easily substituted with other divalent metal ions, and some of these metal-substituted carbonic anhydrases are known to be effective for the hydration of CO_2. The order of the relative activities reported is as follows: Zn(II) > Co(II) ≫ Ni(II) ≈ Mn(II) > Cu(II) ≈ 0.[18] However, because of the serious lack of information on the structure and reactivity of the hydroxo intermediate, the interpretation on the order of the catalytic activity has not been clearly addressed yet.

The high reactivity of the hydroxo copper(II) complex $[Cu(HB(3,5\text{-}iPr_2pz)_3)]_2(OH)_2$ for the fixation of CO_2,[5] together with the inorganic and bioinorganic perspectives described above, inspired us to extend the chemistry to other first-row divalent metal ions including iron and zinc. In this paper, we describe the syntheses and structures of a series of hydroxo complexes of Mn(II), Fe(II), Co(II), Ni(II), Cu(II), and Zn(II) with the tripodal nitrogen ligand $HB(3,5\text{-}iPr_2pz)_3$ (hydrotris(3,5-diisopropyl-1-pyrazolyl)borate). The reactions of these hydroxo complexes with CO_2, without exception, resulted in the formation of μ-carbonato dinuclear complexes. The characterizations and molecular structures of the μ-carbonato complexes are also presented in this paper. The X-ray structures of the hydroxo complexes of Mn,[19] Fe,[20] and Cu[8] and the μ-carbonato dinuclear Cu complex[5] have been communicated previously.

Results and Discussion

Syntheses and Properties of the Hydroxo Complexes. The high reactivity of $[Cu(HB(3,5\text{-}iPr_2pz)_3)]_2(OH)_2$ (**5**) for the fixation of CO_2 is ascribed to the strong electron-donating property of the ligand $HB(3,5\text{-}iPr_2pz_3)$[21] which enhances the nucleophilicity of the coordinated hydroxide. Therefore, our initial efforts have been focused on the synthesis of a series of hydroxo complexes of the divalent metal ions with $HB(3,5\text{-}iPr_2pz)_3$. As reported previously, **5** was prepared by treating a monomeric copper(II) halide complex $Cu(X)(HB(3,5\text{-}iPr_2pz)_3)$ (X = Cl or Br)[22] with 1 N aqueous NaOH.[8] In a similar manner, the hydroxo complexes of Mn(II) (**1**), Co(II) (**3**), and Ni(II) (**4**) were successfully synthesized by treating toluene solutions of the monomeric chloro complexes $M(Cl)(HB(3,5\text{-}iPr_2pz)_3)$ with 1 N aqueous NaOH. The chloro complexes were simply obtained by the reactions of the metal salts MCl_2 with $KHB(3,5\text{-}iPr_2pz)_3$ in an appropriate solvent. For preparing **3**, we noted that $Co(NO_3)(HB(3,5\text{-}iPr_2pz)_3)$ is superior as a starting complex to the chloro complex, because the yield and crystallinity of the nitrate complex are more advantageous. Whereas these hydroxo complexes were easily prepared, preparations of **2** and **6** were not effected by the same reaction method. For instance, the reaction of $Fe(Cl)(HB(3,5\text{-}iPr_2pz)_3)$ or $Zn(Br)(HB(3,5\text{-}iPr_2pz)_3)$ with 1 N aqueous NaOH did not proceed smoothly, and the prolonged reaction merely resulted in decomposition of the halide complex. However, when carboxylato complexes $Fe(OBz)(HB(3,5\text{-}iPr_2pz)_3)$[23] (OBz = benzoato) and $Zn(OAc)(HB(3,5\text{-}iPr_2pz)_3)$ (OAc = acetato) were employed, the acidic ligand reacts with NaOH readily to afford the corresponding hydroxo complexes. In these reactions, relatively dilute aqueous NaOH solutions (0.1–0.5 N) were used in order to avoid decomposition of the complexes. $Fe(OBz)(HB(3,5\text{-}iPr_2pz)_3)$ was prepared by the ligand replacement reaction of $Fe(Cl)(HB(3,5\text{-}iPr_2pz)_3)$ with NaOBz,[23] while $Zn(OAc)(HB(3,5\text{-}iPr_2pz)_3)$ was obtained directly from $Zn(OAc)_2$ and $KHB(3,5\text{-}iPr_2pz)_3$.

All hydroxo complexes **1**–**6** except **2** give rise to the characteristic IR band attributable to ν(OH) at ca. 3700 cm^{-1}; no accurate band was identified for **2**, presumably due to its fast decomposition during the measurement under aerobic conditions. As ascertained by X-ray analyses (*vide infra*), the hydroxo complexes other than **6** possess a dinuclear structure. Accordingly, these dinuclear complexes exhibit characteristic spectroscopic properties associated with the dinuclear structures as follows. Whereas the FD-MS spectra of the complexes do not show the molecular ion, they all give rise to the strong peak attributable to $[M(HB(3,5\text{-}iPr_2pz)_3)]_2O$, presumably resulting from the dissociation of water from the molecular ion during the field

(12) (a) Lorimer, G. H. *Annu. Rev. Plant Physiol.* **1981**, *32*, 349. (b) Miziorko, H. M.; Lorimer, G. H. *Annu. Rev. Biochem.* **1983**, *52*, 507.

(13) (a) Andersson, I.; Knight, S.; Schneider, G.; Lindqvist, Y.; Lundqvist, T.; Brändén, C.-I.; Lorimer, G. H. *Nature (London)* **1989**, *337*, 229. (b) Lundqvist, T.; Schneider, G. *Biochemistry* **1991**, *30*, 904.

(14) (a) Vermaas, W. F.; Govindjee *Photochem. Photobiol.* **1981**, *34*, 775. (b) Diner, B.; Petrouleas, V. *Biochim. Biophys. Acta* **1987**, *895*, 107. The structure of the non-heme iron at the photosynthetic reaction center has been determined: Deisenhofer, J.; Epp, O.; Miki, K.; Huber, R.; Michel, H. *Nature (London)* **1985**, *318*, 618.

(15) Anderson, B. F.; Baker, H. M.; Dodson, E. J.; Norris, G. E.; Rumball, S. V.; Waters, J. M.; Baker, E. N. *Proc. Natl. Acad. Sci. U.S.A.* **1987**, *84*, 1769.

(16) (a) Bertini, I. *Struct. Bonding* **1982**, *48*, 45. (b) Lindskog, S. In *Zinc Enzymes*; Bertini, I., Luchinat, C., Maret, W., Zeppezauer, M., Eds.; Birkhauser: Boston, 1986; p 307.

(17) (a) Kannan, K. K.; Notstrand, B.; Fridborg, K.; Lövgren, S.; Ohlsson, A.; Petef, M. *Proc. Natl. Acad. Sci. U.S.A.* **1975**, *72*, 51. (b) Liljas, A.; Kannan, K. K.; Bergstén, P.-C.; Waara, I.; Fridborg, K.; Strandberg, B.; Carlbom, U.; Järup, L.; Lövgren, S.; Petef, M. *Nature New Biol.* **1972**, *235*, 131.

(18) (a) Lindskog, S.; Malmström, B. G. *J. Biol. Chem.* **1962**, *237*, 1129. (b) Coleman, J. E. *Nature (London)* **1967**, *214*, 193. (c) Thorslund, A.; Linskog, S. *Eur. J. Biochem.* **1967**, *3*, 117.

(19) Kitajima, N.; Singh, U. P.; Amagai, H.; Osawa, M.; Moro-oka, Y. *J. Am. Chem. Soc.* **1991**, *113*, 7757.

(20) Kitajima, N.; Tamura, N.; Tanaka, M.; Moro-oka, Y. *Inorg. Chem.* **1992**, *31*, 3342.

(21) Kitajima, N.; Fujisawa, K.; Fujimoto, C.; Moro-oka, Y. *Chem. Lett.* **1989**, 421.

(22) Kitajima, N.; Fujisawa, K.; Moro-oka, Y. *J. Am. Chem. Soc.* **1990**, *112*, 3210.

(23) Kitajima, N.; Fukui, H.; Moro-oka, Y.; Mizutani, Y.; Kitagawa, T. *J. Am. Chem. Soc.* **1990**, *112*, 6402.

Table I. Magnetic Moments of $LM(\mu\text{-}OH)_2ML$ and $LM(\mu\text{-}CO_3)ML$

complex	found: $\mu_{eff}[\mu_B/M^{2+}]$ ($\mu_{eff}[\mu_B/mol]$)	calcd: $\mu_{spin\ only}$ $[\mu_B/M^{2+}]$
$LMn(\mu\text{-}OH)_2MnL$ (**1**)	4.86 (6.88)	5.92
$LMn(\mu\text{-}CO_3)MnL$ (**7**)	5.32 (7.53)	
$LFe(\mu\text{-}OH)_2FeL$ (**2**)	4.74 (6.71)	4.90
$LFe(\mu\text{-}CO_3)FeL$ (**8**)	4.92 (6.96)	
$LCo(\mu\text{-}OH)_2CoL$ (**3**)	4.40 (6.23)	3.87
$LCo(\mu\text{-}CO_3)CoL$ (**9**)	4.13 (5.84)	
$LNi(\mu\text{-}OH)_2NiL$ (**4**)	2.50 (3.54)	2.83
$LNi(\mu\text{-}CO_3)NiL$ (**10**)	2.30 (3.25)	
$LCu(\mu\text{-}OH)_2CuL$ (**5**)	1.46 (2.06)	1.73
$LCu(\mu\text{-}CO_3)CuL$ (**11**)	0.38 (0.53)	

desorption treatment. Other characteristic peaks observed for these dinuclear hydroxo complexes are the peaks assignable to $[M(HB(3,5\text{-}iPr_2pz)_3)]_2^{2+}$ and $[M(HB(3,5\text{-}iPr_2pz)_3)]_2(CO_3)$. The latter peak should be due to the reaction of the hydroxo complex with atmospheric CO_2 during the mounting of the hydroxo complexes on filaments for FD-MS experiments under aerobic conditions. On the contrary, the hydroxo complex of Zn (**6**) gave no peaks attributable to $[Zn(HB(3,5\text{-}iPr_2pz)_3)]_2(OH)_2$, $[Zn(HB(3,5\text{-}iPr_2pz)_3)]_2O$, or $[Zn(HB(3,5\text{-}iPr_2pz)_3)]_2^{2+}$. Instead, it gives a strong peak at 530 assigned to $[Zn(HB(3,5\text{-}iPr_2pz)_3)]^+$, leading us to favor the monomeric structure of **6**. Another notable feature of the dinuclear hydroxo complexes **1–5** is their magnetic properties associated with the magnetic coupling between the two high-spin metal centers mediated by a bis(μ-hydroxo) bridge. As summarized in Table I, the magnetic susceptibilities of the powdered samples of **1**, **2**, **4**, and **5** are less than those calculated for high-spin dimeric complexes magnetically uncoupled, implying that these complexes are essentially antiferromagnetic. On the other hand, the Co hydroxo complex **3** exhibits a relatively large magnetic susceptibility, possibly indicative of the ferromagnetic property. However, because the value is in the range of the values expected for uncoupled Co(II) dinuclear complexes, a variable-temperature susceptibility measurement is required to evaluate this point clearly. The dimeric complexes **2–5** give rise to isotropically shifted ^{1}H-NMR spectra, although some of the signals are considerably broadened (or cannot be detected).

Complex **2** is extremely oxygen-sensitive. It reacts with dioxygen even at −78 °C instantaneously, though the structure of the oxidized product has not been clarified yet.[20] Complex **1** is moderately oxygen-sensitive, the aerobic oxidation affording two products mainly: a di(μ-oxo)dimanganese(III,III) complex ($[Mn(HB(3,5\text{-}iPr_2pz)_3)]_2(O)_2$) and a mono($\mu$-oxo)manganese-(III,III) complex in which two isopropyl groups are hydroxylated and coordinated to the manganese as an alkoxo ligand. The details of the structures of the oxidized products and the reaction mechanism were described elsewhere.[19,24] The other complexes **3–6** are reasonably stable against dioxygen.

X-ray Crystal Structures of the Hydroxo Complexes. The crystal structures of **1–5** were determined by X-ray crystallography. The structures of **1**, **2**, and **5** were reported previously.[8,19,20] The ORTEP views of **3** and **4** are presented in Figure 2, and the structural parameters are summarized in Table II. In both cases, there are two independent molecules which sit on the crystallographically imposed center of symmetry. Both complexes adopt an essentially very similar dinuclear structure solely bridged with two hydroxo ligands, each metal ion being five-coordinate with a N_3O_2 ligand-donor set. The expanded views of the M–$(OH)_2$–M units of **1–5** are given in Figure 3. The coordination geometry of each metal ion in **1–4** is best described as square-pyramidal. On the other hand, the structure of **5**, which does not contain a center of symmetry, is apparently distinct from those of **1–4**. While the geometry of the copper in **5** is also described as square-pyramidal, the distances between the copper and the apical nitrogen atom from the tris(pyrazolyl)borate ligand (Cu1–N1, 2.37 Å; Cu2–N4, 2.64 Å) are considerably elongated, indicating stronger tetragonality of the ligand field. The apical nitrogen atoms relate to one another in a cis configuration. The distinctive structure of **5** reflects the strong peculiarity of copper(II) ion to favor a tetragonal coordination geometry. On the other hand, it is known that the other divalent metal ions Mn(II), Fe(II), and Co(II) do not prefer tetragonal geometry particularly strongly, while Ni(II) may have such a tendency. Unfortunately, the single crystals of **6** could not be obtained because of its extremely high solubility in most solvents, including pentane. However, on the basis of the FD-MS result described already, we infer that **6** is monomeric by analogy with the hydroxo zinc complex Zn(OH)-(HB(3-tBu-5-Mepz)$_3$), whose crystal structure was very recently reported by Vahrenkamp and Parkin, et al.[6]

Scheme I

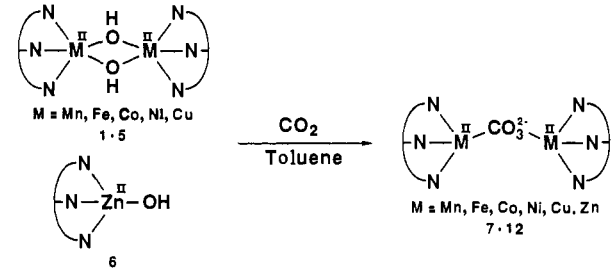

Formation of Dinuclear μ-Carbonato Complexes by CO_2 Fixation with the Hydroxo Complexes. As we reported already, **5** reacts with CO_2 instantaneously to give the (μ-carbonato)-dicopper complex $[Cu(HB(3,5\text{-}iPr_2pz)_3)]_2(CO_3)$ (**11**).[5] Similarly, the hydroxo complexes **1–4** and **6** were found to react with CO_2 to afford μ-carbonato dinuclear complexes **7–10** and **12**, respectively (Scheme I). When the toluene solutions of **3–5** were exposed to 1 atm of CO_2, pronounced color changes were noted due to the formation of the carbonato complexes: Co, **3** → **9**: red → blue purple; Ni, **4** → **10**: yellowish green → emerald green; Cu, **5** → **11**: blue → green. For **1**, **2**, and **6**, the formation of the carbonato complexes is not evident from the color change, since both the starting complexes and the products are colorless. Therefore, in these reactions, the formation of the carbonato complexes was established on the basis of spectroscopic data including NMR and FD-MS and X-ray structural analyses. All μ-carbonato complexes give rise to the distinct peak corresponding to the molecular ion in the FD-MS spectra, supporting the dinuclear μ-carbonato structures. In particular, the structure of the diamagnetic carbonato complex **12** was fully characterized by ^{1}H- and ^{13}C-NMR spectroscopy. The notable feature of the complex is the signal observed at 171 ppm attributable to the carbonate carbon. Several examples of diamagnetic μ-carbonato dinuclear metal complexes are known.[25] The ^{13}C-NMR chemical shifts of the carbonate carbon reported for these complexes are located in the range of 169–172 ppm. Hence, the value of **12** is typical for the structure.

X-ray Structures of the μ-Carbonato Complexes. Although all attempts to prepare single crystals of the (μ-carbonato)manganese complex **7** were unsuccessful, the crystal structures of the other μ-carbonato complexes **8–12** were determined by X-ray crystallography. The ORTEP views and the expanded details of the N_3M–(CO_3)–MN_3 moieties of **8–12** are given in Figures 4 and 5, respectively. The selected bond lengths and angles are summarized in Table III. All complexes possess dinuclear structures as we suggested on the basis of the spectroscopic data

(24) Kitajima, N.; Osawa, M.; Tanaka, M.; Moro-oka, Y. *J. Am. Chem. Soc.* **1991**, *113*, 8952.

(25) (a) Strom, E. T.; Woessner, D. E.; Smith, W. B. *J. Am. Chem. Soc.* **1981**, *103*, 1255. (b) Yoshida, T.; Youngs, W. J.; Sakaeda, T.; Ueda, T.; Otsuka, S.; Ibers, J. A. *J. Am. Chem. Soc.* **1983**, *105*, 6273. (c) Lundquist, E. G.; Folting, K.; Huffman, J. C.; Caulton, K. G. *Inorg. Chem.* **1987**, *26*, 205. (d) Brücher, E.; Glaser, J.; Toth, I. *Inorg. Chem.* **1991**, *30*, 2239.

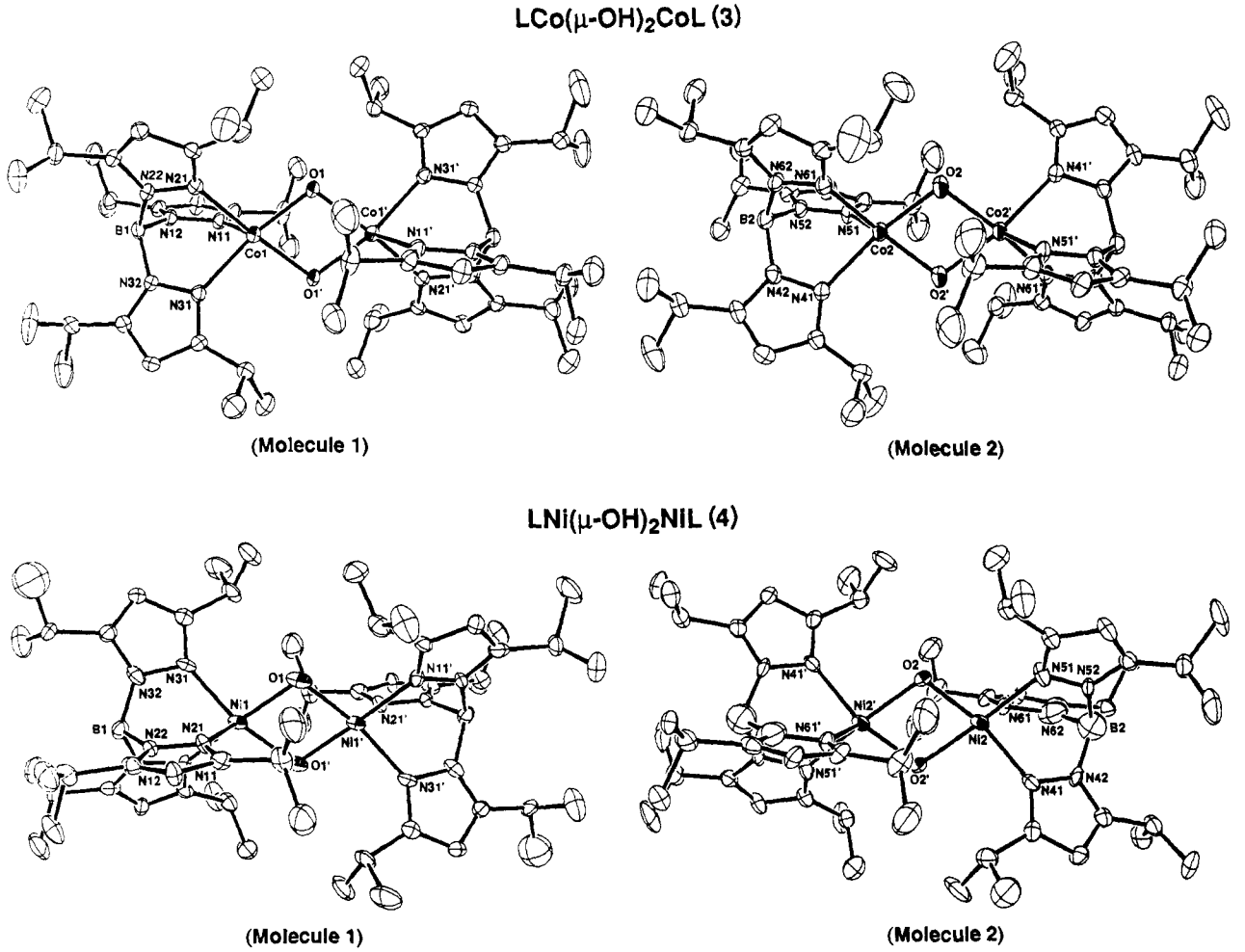

Figure 2. ORTEP views of bis(μ-hydroxo) complexes of Co (**3**) and Ni (**4**) (30% probability). Two independent molecules sit on a crystallographically imposed center of symmetry. The pentane molecules of crystallization are omitted for clarity.

described above. A variety of coordination modes of the carbonate group is seen. The complexes of Ni (**10**) and Cu (**11**) contain a carbonate group which is bound to each metal ion tightly in a bidentate coordination mode. The coordination modes of the carbonate in these complexes are virtually symmetric, since all M–O bonds are comparable. In the complexes of Fe (**8**) and Co (**9**), however, the coordination geometries are rather unsymmetric, though the carbonate groups are still coordinated to both metal ions bidentately. Accordingly, one of the M–O1 bonds, where O1 denotes the oxygen atom of the carbonate group sitting between the two metal centers, is more elongated (ca. 2.27 Å) than the other (ca. 2.06 Å). Also, the bond distances between the metal and the carbonato oxygens (O2 or O3), which are terminally bound to one side metal ion, are not equal: Co1–O2 (2.09 Å) vs Co2–O3 (1.99 Å); Fe2–O3 (2.11 Å) vs Fe1–O2 (2.01 Å). The distortion of the carbonate coordination is even more pronounced for the zinc complex **12**. In **12**, the carbonate group is bound to Zn1 in a bidentate coordination mode and unidentately to Zn2. The N_3O_2 ligand field around Zn1 is very distorted because the distance between the zinc and one oxygen from the carbonate is significantly elongated (2.34 Å), while other Zn–N and Zn–O bond lengths are almost comparable (1.98–2.07 Å). The synthesis and structural determination of the μ-carbonato complex **12** were independently accomplished by Parkin et al. very recently.[26] The crystal structures are essentially identical; the crystal Parkin et al. obtained contains solvent of recrystallization (benzene) and gives rise to a different space group. As a related complex to **12**, Parkin and Vahrenkamp, et al., reported the crystal structure of $[Zn(HB(3\text{-}tBu\text{-}5\text{-}Mepz)_3)]_2(CO_3)$, which was also prepared by treating a hydroxo zinc complex[6] with CO_2.[26,27] The coordination mode of the complex is, however, distinctive from that of **12**; in $[Zn(HB(3\text{-}tBu\text{-}5\text{-}Mepz)_3)]_2(CO_3)$, the carbonate group is bound to both zinc ions unidentately. This structural inconsistency reflects the steric hindrance of the tris(pyrazolyl)borate ligand. The hindrance of $HB(3\text{-}tBu\text{-}5\text{-}Mepz)_3$ is apparently larger than that of $HB(3,5\text{-}iPr_2pz)_3$.

The X-ray structures of the series of the μ-carbonato complexes **8**–**12** established that the distortions of the coordination mode of the carbonato group are in the following order: Zn > Co ≈ Fe > Ni ≈ Cu. Similar geometric distortions which depend upon the metal center have recently been pointed out by Parkin et al.[26,28] in their comparison of the crystal structures of a series of monomeric nitrate complexes $M(NO_3)(HB(3\text{-}tBupz)_3)$ (M(II) = Co, Ni, Cu, Zn). The order of the distortion is also Zn (unidentate) > Co (asymmetric bidentate) > Cu = Ni (symmetrical bidentate). Here, it is noteworthy that the order, as demonstrated by Parkin et al.,[26,28] is mostly correlated with that of the catalytic activities of metal-substituted carbonic anhydrases (Zn > Co ≫ Mn ≈ Ni > Cu ≈ 0).

Infrared Spectra and Magnetic Properties of the μ-Carbonato Complexes. IR spectroscopy is a traditional means of ascertaining the coordination mode of the carbonate group. For instance, ν_3 and ν_4, which are doubly degenerate in free carbonate ion (D_{3h}), are split into two when the carbonate ion is coordinated to a metal ion. In general, the splitting of the degenerate vibrations

(26) Han, R.; Looney, A.; McNeill, K.; Parkin, G.; Rheingold, A. L.; Haggerty, B. S. *J. Inorg. Biochem.* **1993**, *49*, 105.

(27) Looney, A.; Parkin, G.; Alsfasser, R.; Ruf, M.; Vahrenkamp, H. *Angew. Chem., Int. Ed. Engl.* **1992**, *31*, 92.

(28) Han, R.; Parkin, G. *J. Am. Chem. Soc.* **1991**, *113*, 9707.

Table II. Selected Bond Distances (Å) and Bond Angles (deg) for $[Co(HB(3,5\text{-}iPr_2pz)_3]_2(OH)_2\cdot 2C_5H_{12}$ (**3**·$2C_5H_{12}$) and $[Ni(HB(3,5\text{-}iPr_2pz)_3]_2(OH)_2\cdot 2C_5H_{12}$ (**4**·$2C_5H_{12}$)

		$LCo(\mu\text{-}OH)_2CoL\cdot 2C_5H_{12}$ (**3**·$2C_5H_{12}$)			
		Bond Distances			
Co1–O1	2.024(7)	Co2–N41	2.17(1)	Co1–Co1′	3.202(3)
Co1–N11	2.080(9)	Co2–N61	2.119(6)	Co2–O2′	2.03(1)
Co1–N31	2.137(7)	Co1–O1′	2.011(5)	Co2–N51	2.089(7)
Co2–O2	1.971(5)	Co1–N21	2.189(7)	Co2–Co2′	3.189(3)
		Bond Angles			
O1–Co1–O1′	75.0(3)	O2′–Co2–N41	163.6(3)	N11–Co1–N31	88.3(3)
O1–Co1–N11	109.4(3)	O2′–Co2–N61	95.4(3)	O2–Co2–O2′	74.5(3)
O1–Co1–N31	98.3(3)	N41–Co2–N61	84.8(3)	O2–Co2–N41	97.5(3)
O1′–Co1–N21	96.5(2)	Co1–O1–Co1′	105.0(3)	O2–Co2–N61	151.1(3)
N11–Co1–N21	90.4(3)	O1–Co1–N21	160.1(3)	O2′–Co2–N51	110.8(3)
N21–Co1–N31	83.1(2)	O1′–Co1–N11	112.8(3)	N41–Co2–N51	85.5(3)
Co2–O2–Co2′	105.5(3)	O1′–Co1–N31	158.9(3)	N51–Co2–N61	91.4(2)
O2–Co2–N51	117.5(3)				
		$LNi(\mu\text{-}OH)_2NiL\cdot 2C_5H_{12}$ (**4**·$2C_5H_{12}$)			
		Bond Distances			
Ni1–O1	1.983(5)	Ni2–N41	2.103(6)	Ni1–Ni1′	3.204(3)
Ni1–N11	2.164(7)	Ni2–N61	2.070(7)	Ni2–O2′	2.041(9)
Ni1–N31	2.077(7)	Ni1–O1′	2.026(7)	Ni2–N51	2.16(1)
Ni2–O2	1.957(5)	Ni1–O21	2.096(9)	Ni2–Ni2′	3.197(4)
		Bond Angles			
O1–Ni1–O1′	73.9(3)	O2′–Ni2–N41	95.4(3)	N11–Ni1–N31	85.6(3)
O1–Ni1–N11	97.4(2)	O2′–Ni2–N61	108.5(4)	O2–Ni2–O2′	73.8(3)
O1–Ni1–N31	160.4(4)	N41–Ni2–N61	91.7(3)	O2–Ni2–N41	157.0(3)
O1′–Ni1–N21	107.4(3)	Ni1–O1–Ni1′	106.1(3)	O2–Ni2–N61	110.8(3)
N11–Ni1–N21	90.7(3)	O1–Ni1–N21	110.9(3)	O2′–Ni2–N51	164.2(3)
N21–Ni1–N31	88.4(3)	O1′–Ni1–N11	161.7(3)	nN41–Ni2–N51	86.2(3)
Ni2–O2–Ni2′	106.2(3)	O1′–Ni1–N31	97.5(3)	N51–Ni2–N61	87.1(4)
O2–Ni2–N51	98.9(3)				

is larger in the bidentate coordination mode than in the unidentate.[29] However, no simple criterion has been established to gain further details of the coordination structure. Yet, in the series of the μ-carbonato dinuclear complexes synthesized and structurally determined in the present work, the C–O asymmetrical stretching band of the μ-carbonato complexes reflects the coordination mode of the carbonato group. Other IR bands due to the carbonate group are, unfortunately, not clearly identified owing to the overlapping bands due to the $HB(3,5\text{-}iPr_2pz)_3$. The symmetric carbonato complexes **10** and **11** give a sharp band at ca. 1580–1590, whereas asymmetric complexes **8** and **9** give a broad band at ca. 1650–1550 cm^{-1}. The band of **12** is particularly broadened and observed as a shoulder at ca. 1700–1520 cm^{-1}. On the basis of this criterion, the Mn complex **7** possesses an asymmetric bidentate coordination mode of the carbonate, similar to the Fe (**8**) and Co (**9**) complex.

As expected for the dinuclear structures, the complexes **7**–**11** are antiferromagnetic or ferromagnetic owing to the magnetic interaction through the μ-carbonate group. The antiferromagnetic properties of **7**, **10**, and **11** are evident from the relatively low magnetic susceptibilities which are listed in Table I. The magnetism of carbonato complexes as well as bis(μ-hydroxo) complexes may be correlated with the coordination structures revealed by X-ray crystallography. The complexes of Ni (**10**) and Cu (**11**), both containing a symmetrically bidentate carbonate, exhibit smaller magnetic susceptibilities than the corresponding bis(μ-hydroxo) complexes **4** and **5**. This is ascribed to the stronger antiferromagnetic coupling through the bridging oxygen of the carbonate group than that mediated by a bis(hydroxo) bridge, presumably because the M–O–M angles in the carbonato complexes are close to linear (176–178°). On the other hand, with an unsymmetric coordination mode, the carbonate group does not mediate the magnetic interaction very effectively, since one side M–O bond is significantly elongated. Accordingly, the magnetic susceptibilities of Mn (**7**) and Fe (**8**) are higher than those of the corresponding bis(μ-hydroxo) complexes **1** and **2**. Fe (**8**) and Co (**9**) carbonato complexes exhibit magnetic susceptibilities near the spin only values, indicative of no significant magnetic coupling in these complexes.

Relative Capabilities of the Hydroxo Complexes for Fixing CO_2. All hydroxo complexes were found to react with atmospheric CO_2, resulting in the formation of the corresponding μ-carbonato complexes. A representative example of fixation of atmospheric CO_2 is shown in Figure 6, where the time-dependent change of the electronic spectra of (μ-hydroxo)cobalt complex **3** under air is presented. The spectrum of **3** gives characteristic bands at 453, 551, and 730 nm. When the solution was exposed to air and allowed to stand at 25 °C, the intensities of the bands due to **3** decreased gradually, while another intense band appeared at 572 nm, which is attributable to the μ-carbonato complex **9**. The intensity of the band due to **9** reached the maximum within 48 h, and from the maximum intensity it was concluded that **9** is formed from **3** quantitatively with atmospheric CO_2. The formation of **9** from **3** with atmospheric CO_2 was further confirmed by IR and ^{1}H-NMR spectroscopy. Figure 7 shows the time dependent ^{13}C-NMR spectra of the hydroxo Zn complex **6** recorded in a sealed NMR tube under air. It is evident that a signal at 171 ppm assigned to the carbonate ion in **12** develops with time, indicating that **6** reacts with atmospheric CO_2 to give **12**, though the CO_2 amount in the sealed tube is not enough for complete conversion of **6** to **12**, and thus the rate of conversion is very slow. No signal other than the ones due to **6** and **12** was observed during the reaction. This implies that once **6** reacts with CO_2, the resulting bicarbonate species, the most plausible intermediate, should immediately undergo a subsequent reaction with another **6** to afford **12**.

The capabilities of the series of hydroxo complexes for fixing CO_2 were explored and compared. The rates were determined by time-dependent changes of the electronic spectra for the complexes of Co (**3**), Ni (**4**), and Cu (**5**) in the presence of an appropriate concentration of CO_2 because they exhibit characteristic absorption bands in the visible region. The formation

(29) Nakamoto, K. *Infrared and Raman Spectra of Inorganic and Coordination Compounds*, 4th ed.; John Wiley & Sons: New York, 1986.

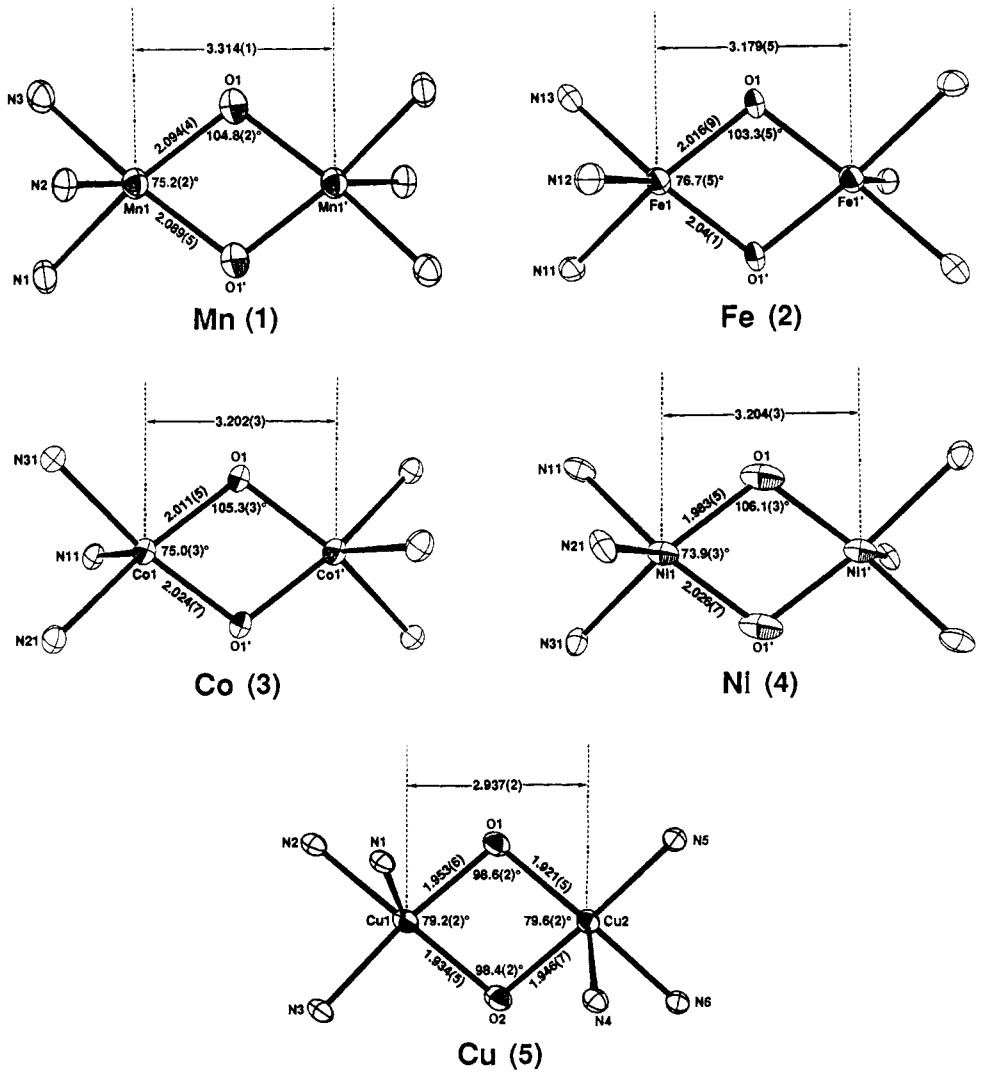

Figure 3. Expanded views of the metal coordination spheres of bis(μ-hydroxo) complexes of Mn (**1**), Fe (**2**), Co (**3**), Ni (**4**), and Cu (**5**). One of crystallographically independent molecules of **2**, **3**, or **4** is presented.

rate of the Zn complex **6**, which is colorless, was established by ^{1}H-NMR spectroscopy. To compare the rate with others, the ^{1}H-NMR experiments were performed for **4** and **5** under the same reaction conditions. The relative rate of the Mn complex **1** to that of the Co complex **4** was evaluated by FT-IR, because **1** is colorless and NMR inactive. Finally, the rate of the Fe complex **2** was estimated by ^{1}H-NMR spectroscopy. More details of the experimental methods to evaluate the relative rates are provided in the Experimental Section. These experiments led us to conclude the order of activities of the series of the hydroxo complexes to react with CO_2 as follows: Zn > Cu > Ni $\approx$ Co > Mn > Fe. Since all hydroxo complexes except the Zn complex **6** possess a similar dinuclear structure and the reaction conditions are comparable, the order of activities merely reflects the nucleophilicity of the hydroxide ion, which should be affected by the electronic property of the central metal. The noteworthy aspect is that the order is different from the order of activities known for metal-substituted carbonic anhydrases for hydration of CO_2. In particular, the Cu complex **5** is very effective for CO_2 fixation, while copper-substituted carbonic anhydrase was reported to be ineffective for CO_2 hydration.[18]

Hydration of the μ-Carbonato Complexes. In order to elucidate the accessibilities of the carbonato complexes to hydration, we examined the reaction of the μ-carbonato complex with water or aqueous NaOH. None of the μ-carbonato complexes were converted into the hydroxo complex when they were simply stirred in toluene in the presence of water. However, when the carbonato

Scheme II

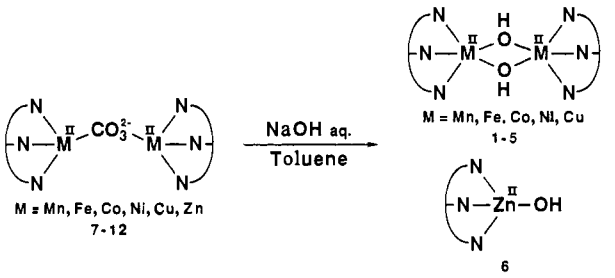

complexes were treated with 1 N aqueous NaOH for 2 h in toluene under argon, all carbonato complexes **7–12** were converted to the hydroxo complexes **1–6**, respectively (Scheme II). The rates of the hydrolysis of (μ-carbonato)cobalt (**9**) and -copper (**11**) complexes into the hydroxo complexes are compared by electronic spectroscopy. As indicated in Figure 8, the solution color of **9** changed with time in the presence of aqueous NaOH under Ar. The final features of the spectrum are identical to those of the hydroxo complex **3**, indicating the quantitative formation of **3** from **9**. The complete conversion required 7 h. The same experiment was applied to **11**. Under the same conditions, even after 12 h, the conversion of **11** to **5** was not complete. This established that **9** is more facilely hydrolyzed to the hydroxo complex than **11**.

From Schemes I and II, a metal-catalyzed fixation of

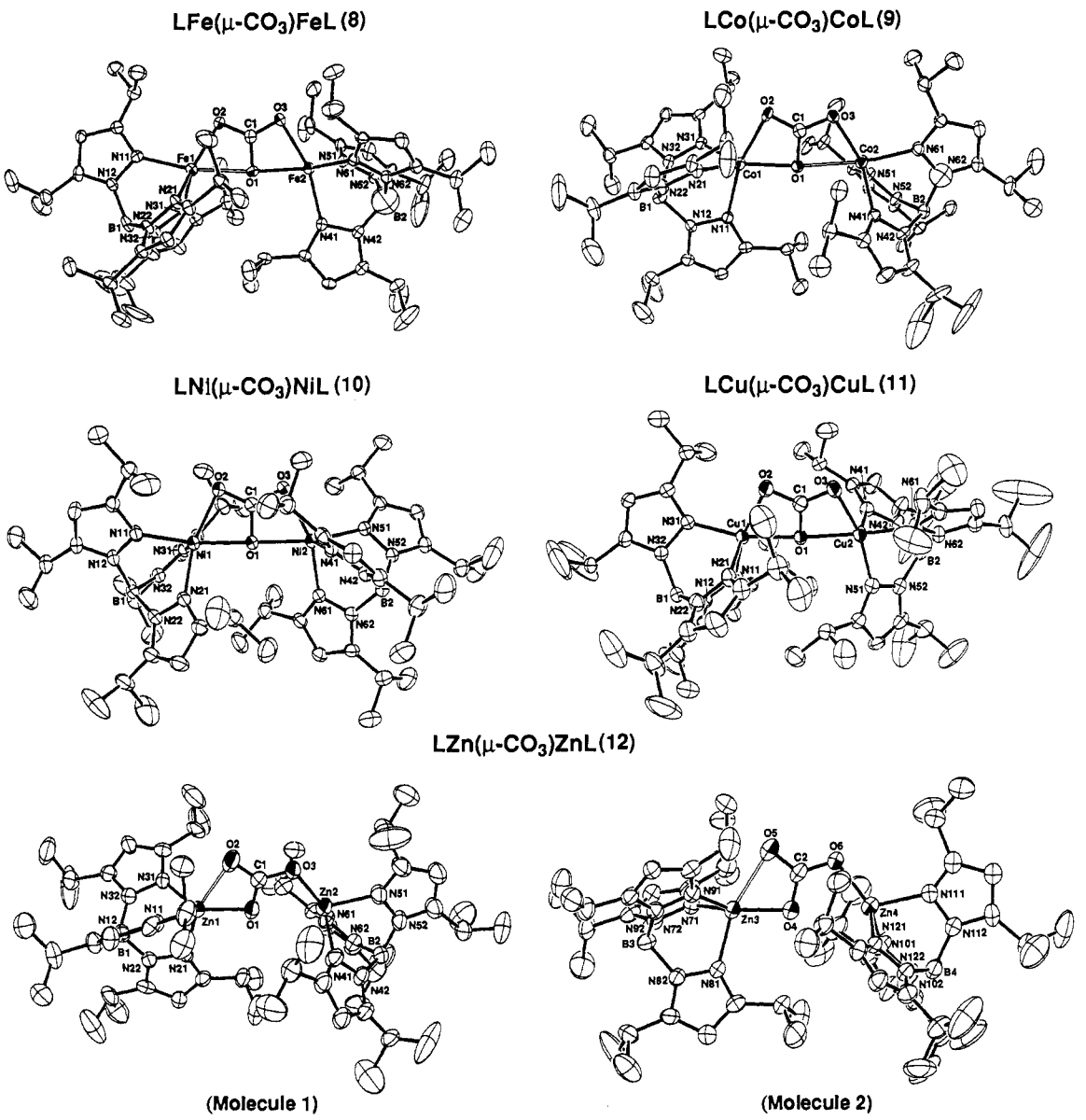

Figure 4. ORTEP views of μ-carbonato complexes of Fe (**8**), Co (**9**), Ni (**10**), Cu (**11**), and Zn (**12**) (30% probability). The solvent molecules of crystallization are omitted for clarity.

atmospheric CO_2, the overall reaction being given as eq 3, is

$$CO_2 + 2NaOH \longrightarrow Na_2CO_3 + H_2O \quad (3)$$

possible, whereas the effectiveness of the present metal complexes is not very high. Development of more effective catalytic systems by designing more suitable ligands is being planned.

Biological Relevance. The mechanism of carbonic anhydrase has been discussed for quite some time. In this section, we do not intend to survey nor to discuss the details of these mechanistic studies, because a number of excellent review articles and theoretical studies are available.[16,30,31] Among a variety of mechanisms proposed, one of the most generally accepted is the hydroxide mechanism.[32] According to this mechanism, water coordinated to the zinc is deprotonated and the resultant zinc hydroxide works as an active species (see Figure 1). One disadvantage of this mechanism was the pK_a value of water coordinated to the zinc ion in carbonic anhydrase (pK_a = ca. 7).[33] Since zinc complexes previously demonstrated as carbonic anhydrase models exhibit pK_as above 8.3,[30,34] the relatively low pK_a value of carbonic anhydrase has been a controversial problem. However, recently Kimura et al.[35] succeeded in preparing an excellent model for carbonic anhydrase, a tetrahedral hydroxo zinc complex with a water-soluble N_3 polyamine ligand and definitely established that the pK_a (7.3) of this complex is comparable to that of carbonic anhydrase. Thus, the difference in pK_a was ascribed mainly to the tetrahedral coordination geometry; most of the zinc complexes investigated previously were not tetrahedral.[30,34]

(30) Kimura, E.; Koike, T. *Comments Inorg. Chem.* **1991**, *11*, 285.
(31) (a) Cook, C. M.; Haydock, K.; Lee, R. H.; Allen, L. C. *J. Phys. Chem.* **1984**, *88*, 4875. (b) Liang, J.-Y.; Lipscomb, W. N. *Biochemistry* **1987**, *26*, 5293. (c) Liang, J.-Y.; Lipscomb, W. N. *Biochemistry* **1988**, *27*, 8676. (d) Merz, K. M., Jr.; Hoffman, R.; Dewar, M. J. S. *J. Am. Chem. Soc.* **1989**, *111*, 5636. (e) Jacob, O.; Cardenas, R.; Tapia, O. *J. Am. Chem. Soc.* **1990**, *112*, 8692.
(32) Coleman, J. E. In *Biophysics and Phisiology of Carbon Dioxide*; Bauer, C., Gros, G., Bartels, H., Eds.; Springer: Berlin, 1980; p 133.
(33) (a) Pocker, Y.; Stone, J. T. *J. Am. Chem. Soc.* **1965**, *87*, 5497. (b) Pocker, Y.; Sarkanen, S. *Adv. Enzymol.* **1987**, *47*, 149. (c) Silverman, D. N.; Lindskog, S. *Acc. Chem. Res.* **1988**, *21*, 30.
(34) (a) Wooley, P. *Nature (London)* **1975**, *258*, 677. (b) Wooley, P. *J. Chem. Soc., Perkin Trans. II* **1977**, 318. (c) Groves, J. T.; Dias, R. M. *J. Am. Chem. Soc.* **1979**, *101*, 1033. (d) Groves, J. T.; Chambers, R. R., Jr. *J. Am. Chem. Soc.* **1984**, *106*, 630. (e) Gellman, S. H.; Petter, R.; Breslow, R. *J. Am. Chem. Soc.* **1986**, *108*, 2388. (f) Kimura, E.; Koike, T.; Toriumi, K. *Inorg. Chem.* **1988**, *27*, 3687.
(35) Kimura, E.; Shiota, T.; Koike, T.; Shiro, M.; Kodama, M. *J. Am. Chem. Soc.* **1990**, *112*, 5805.

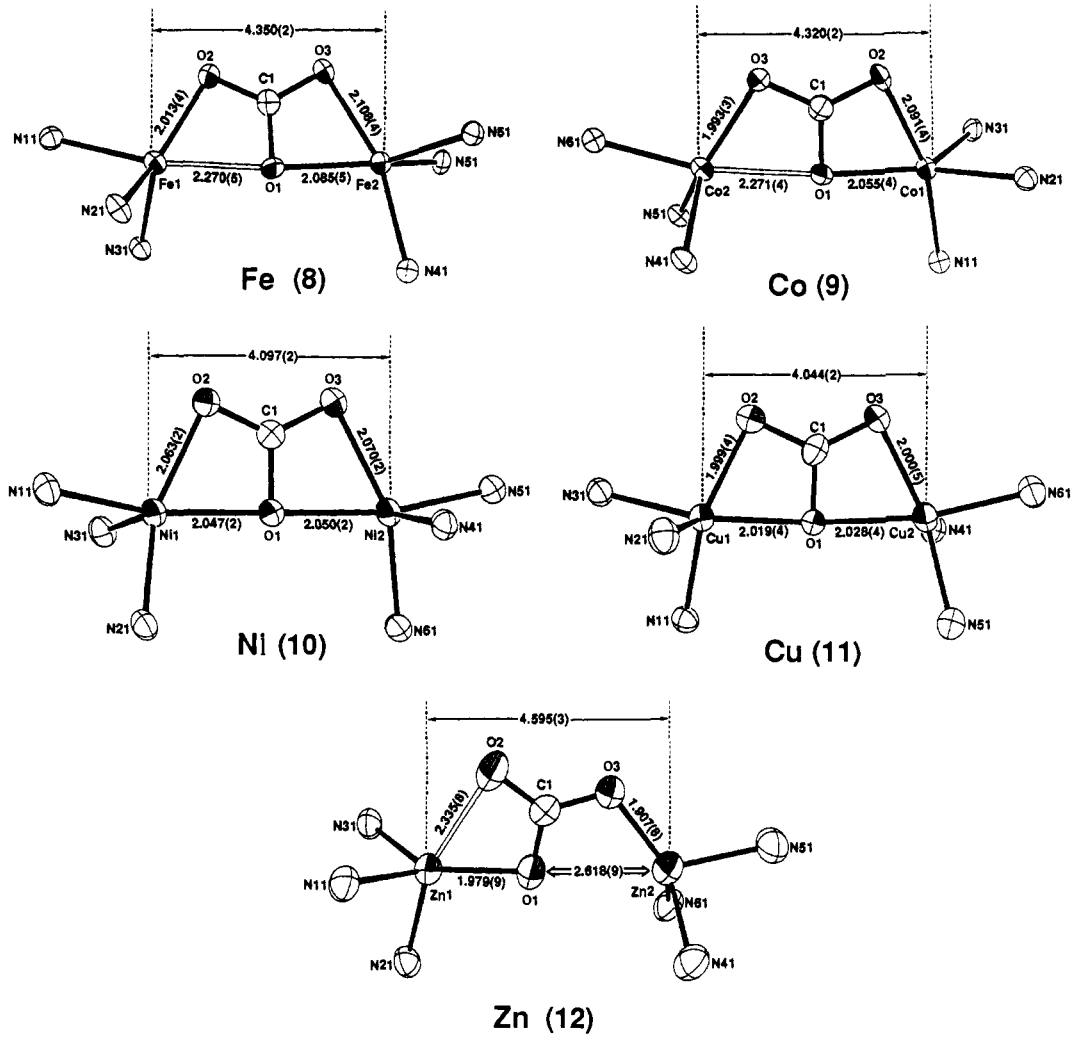

Figure 5. Expanded views of the metal coordination spheres of μ-carbonato complexes of Fe (**8**), Co (**9**), Ni (**10**), Cu (**11**), and Zn (**12**). One of the molecules of **12** is presented.

The present work has focused on the synthesis and structural determination of a series of hydroxo complexes and their reactivities toward CO_2, primarily in the hope of isolating and structurally characterizing the products. Thus we used a hindered N_3 ligand $HB(3,5\text{-}iPr_2pz)_3$ to explore the chemistry under very hydrophobic conditions, e.g., in toluene, in order to avoid the complicated features associated with the ligand displacement and the decomposition of the product. Unfortunately, both the starting hydroxo complexes and CO_2 adducts, μ-carbonato complexes, have been revealed to possess dinuclear structures except the zinc hydroxo complex **6**. Because of differences in nuclearity between the present complexes and the monomeric metal sites in metal-substituted carbonic anhydrases, we should refrain from overstating the biological relevance of the present study to the catalysis of carbonic anhydrase. Yet, we point out two important inorganic aspects which should be taken into account in considering the mechanism of carbonic anhydrase. First, the nucleophilic CO_2 fixation abilities of the series of divalent metal hydroxo complexes are in the following order: Zn > Cu > Ni $\approx$ Co > Mn > Fe. While Zn is the most effective, this order does not fit the one reported for the CO_2 hydration activities of carbonic anhydrases substituted with a series of divalent metal ions: Zn $\gg$ Co > Ni $\approx$ Mn > Cu $\approx$ 0. Because the order of activities might be affected by the solvent, it may be difficult to compare the present results with those of the carbonic anhydrases directly. However, the active site of carbonic anhydrase is known to be hydrophobic. As the order of CO_2 fixation was determined under very hydrophobic conditions, in toluene or benzene, it seems likely that the difference in the order of CO_2 fixing activity between the synthetic hydroxo complexes and metal-substituted carbonic anhydrases is not due to such a side effect. Hence, we suggest that the nucleophilicity of the metal hydroxide formed in carbonic anhydrase does not play a critical role in determining the catalytic activity of carbonic anhydrase.

Second, the order of the coordination distortions observed for the series of μ-carbonato complexes, Zn > Co $\approx$ Fe $\approx$ Mn > Ni $\approx$ Cu, are mostly correlated with the order of activities of metal-substituted carbonic anhydrases. If the unidentately coordinated carbonate (bicarbonate) is more susceptible to hydrolysis with water than the bidentate form, this experimental fact may imply that the dissociation pathway of the formed bicarbonate intermediate is the rate-determining step in the hydration of CO_2 catalyzed by carbonic anhydrase.[28] The experimental result that the symmetric carbonato Cu complex **11** is more inert than unsymmetric carbonato complex **9** for the hydrolysis may provide evidence for this hypothesis. The important role of the proton transfer in the catalysis of carbonic anhydrase was pointed out previously on the basis of kinetic investigations.[36]

Finally we comment on the ineffectiveness of copper-substituted carbonic anhydrase. The Cu(II) hydroxo complex **5** was found to be very effective for CO_2 fixation in the present study. The high effectiveness of Cu(II) complexes for a variety of hydrolytic reactions is well known.[37] Then, the question naturally arises: why is Cu(II) ion ineffective for carbonic anhydrase? One plausible explanation is that the Cu(II)-substituted carbonic

(36) (a) Pocker, Y.; Bjorkquist, D. W. *Biochemistry* **1977**, *16*, 5698. (b) Jonsson, B.-H.; Steiner, H.; Lindskog, S. *FEBS Lett.* **1976**, *64*, 310. (c) Pocker, Y.; Tanaka, N. *Science* **1978**, *199*, 907.

Table III. Selected Bond Distances (Å) and Bond Angles (deg) for $[Fe(HB(3,5\text{-}iPr_2pz)_3)]_2(CO_3)\cdot 2MeCN$ (**8**·2MeCN), $[Co(HB(3,5\text{-}iPr_2pz)_3)]_2(CO_3)\cdot 2MeCN$ (**9**·2MeCN), $[Ni(HB(3,5\text{-}iPr_2pz)_3)]_2(CO_3)\cdot Me_2CO$ (**10**·Me_2CO), $[Cu(HB(3,5\text{-}iPr_2pz)_3)]_2(CO_3)\cdot 2MeCN$ (**11**·2MeCN), and $[Zn(HB(3,5\text{-}iPr_2pz)_3)]_2(CO_3)$ (**12**)

$LFe(\mu\text{-}CO_3)FeL\cdot 2MeCN$ (**8**·2MeCN)

Bond Distances

Fe1–O1	2.270(5)	C1–O1	1.302(7)	Fe2–N41	2.133(5)
Fe2–O1	2.085(5)	C1–O3	1.255(8)	Fe2–N61	2.080(5)
Fe1–N11	2.096(6)	Fe1–O2	2.013(4)	C1–O2	1.276(8)
Fe1–N31	2.070(4)	Fe2–O3	2.108(4)	Fe1–Fe2	4.350(2)
Fe2–N51	2.093(6)	Fe1–N21	2.086(5)		

Bond Angles

O1–Fe1–O2	61.7(2)	N41–Fe2–N61	89.5(2)	N21–Fe1–N31	94.1(2)
O1–Fe1–N21	101.6(2)	Fe1–O1–Fe2	174.4(2)	O1–Fe2–N41	100.3(2)
O2–Fe1–N11	107.1(2)	Fe2–O1–C1	90.6(4)	O1–Fe2–N61	104.5(2)
O2–Fe1–N31	136.7(2)	Fe2–O3–C1	90.8(3)	O3–Fe2–N51	102.8(2)
N11–Fe1–N31	87.5(2)	O1–Fe1–N11	168.3(2)	N41–Fe2–N51	87.6(2)
O1–Fe2–O3	62.4(2)	O1–Fe1–N31	99.0(2)	N51–Fe2–N61	88.4(2)
O1–Fe2–N51	131.7(2)	O2–Fe1–N21	126.3(2)	Fe1–O1–C1	84.2(4)
O3–Fe2–N41	162.6(2)	N11–Fe1–N21	87.6(2)	Fe1–O2–C1	96.4(3)
O3–Fe2–N61	104.5(2)				

$LCo(\mu\text{-}CO_3)CoL\cdot 2MeCN$ (**9**·2MeCN)

Bond Distances

Co1–O1	2.055(4)	C1–O1	1.381(6)	Co2–N41	2.053(3)
Co2–O1	2.271(4)	C1–O3	1.276(6)	Co2–N61	2.051(5)
Co1–N11	2.089(4)	Co1–O2	2.091(4)	C1–O2	1.266(6)
Co1–N31	2.078(4)	Co2–O3	1.993(3)	Co1–Co2	4.320(2)
Co2–N51	2.031(4)	Co1–N21	2.052(4)		

Bond Angles

O1–Co1–O2	63.4(1)	N41–Co2–N61	88.9(2)	N21–Co1–N31	89.9(2)
O1–Co1–N21	131.5(1)	Co1–O1–Co2	174.0(2)	O1–Co2–N41	97.7(1)
O2–Co1–N11	163.9(2)	Co2–O1–C1	83.2(3)	O1–Co2–N61	167.8(1)
O2–Co1–N31	102.7(1)	Co2–O3–C1	96.6(3)	O3–Co2–N51	126.2(1)
N11–Co1–N31	90.2(1)	O1–Co1–N11	100.5(1)	N41–Co2–N51	96.0(2)
O1–Co2–O3	62.3(1)	O1–Co1–N31	137.1(1)	N51–Co2–N61	89.3(2)
O1–Co2–N51	100.2(2)	O2–Co1–N21	101.3(2)	Co1–O1–C1	90.9(3)
O3–Co2–N41	134.6(2)	N11–Co1–N21	88.2(2)	Co1–O2–C1	90.7(3)
O3–Co2–N61	105.8(1)				

$LNi(\mu\text{-}CO_3)NiL\cdot Me_2CO$ (**10**·Me_2CO)

Bond Distances

Ni1–O1	2.047(2)	C1–O1	1.324(4)	Ni2–N41	2.007(3)
Ni2–O1	2.050(2)	C1–O3	1.256(3)	Ni2–N61	2.033(3)
Ni1–N11	2.008(3)	Ni1–O2	2.063(2)	C1–O2	1.269(4)
Ni1–N31	2.017(3)	Ni2–O3	2.070(2)	Ni1–Ni2	4.097(2)
Ni2–N51	2.018(2)	Ni1–N21	2.021(3)		

Bond Angles

O1–Ni1–O2	64.4(1)	N41–Ni2–N61	94.5(1)	N21–Ni1–N31	95.5(1)
O1–Ni1–N21	98.3(1)	Ni1–O1–Ni2	178.0(1)	O1–Ni2–N41	104.3(1)
O2–Ni1–N11	104.6(1)	Ni2–O1–C1	89.4(2)	O1–Ni2–N61	97.1(1)
O2–Ni1–N31	105.7(1)	Ni2–O3–C1	90.4(2)	O3–Ni2–N51	103.9(1)
N11–Ni1–N31	89.2(1)	O1–Ni1–N11	164.7(1)	N41–Ni2–N51	89.8(1)
O1–Ni2–O3	64.1(1)	O1–Ni1–N31	103.8(1)	N51–Ni2–N61	90.4(1)
O1–Ni2–N51	163.4(1)	O2–Ni1–N21	155.1(1)	Ni1–O1–C1	89.6(2)
O3–Ni2–N41	106.1(1)	N11–Ni1–N21	88.3(1)	Ni1–O2–C1	90.4(2)
O3–Ni2–N61	154.8(1)				

$LCu(\mu\text{-}CO_3)CuL\cdot 2MeCN$ (**11**·2MeCN)

Bond Distances

Cu1–O1	2.019(4)	C1–O1	1.310(7)	Cu2–N41	2.253(6)
Cu2–O1	2.028(4)	C1–O3	1.257(7)	Cu2–N61	1.973(5)
Cu1–N11	1.975(5)	Cu1–O2	1.999(4)	C1–O2	1.281(8)
Cu1–N31	1.970(5)	Cu2–O3	2.000(5)	Cu1–Cu2	4.044(2)
Cu2–N51	1.962(5)	Cu1–N21	2.196(6)		

Bond Angles

O1–Cu1–O2	66.0(2)	N41–Cu2–N61	91.0(2)	N21–Cu1–N31	90.2(2)
O1–Cu1–N21	100.0(2)	Cu1–O1–Cu2	175.7(2)	O1–Cu2–N41	99.7(2)
O2–Cu1–N11	158.4(2)	Cu2–O1–C1	87.3(3)	O1–Cu2–N61	165.3(2)
O2–Cu1–N31	101.9(2)	Cu2–O3–C1	90.0(4)	O3–Cu2–N51	161.2(2)
N11–Cu1–N31	90.9(2)	O1–Cu1–N11	98.4(2)	N41–Cu2–N51	92.9(2)
O1–Cu2–O3	65.8(2)	O1–Cu1–N31	165.6(2)	N51–Cu2–N61	88.9(2)
O1–Cu2–N51	100.5(2)	O2–Cu1–N21	103.8(2)	Cu1–O1–C1	88.5(3)
O3–Cu2–N41	101.8(2)	N11–Cu1–N21	93.2(2)	Cu1–O2–C1	90.2(3)
O3–Cu2–N61	102.3(2)				

Table III. (continued)

$LZn(\mu\text{-}CO_3)ZnL$ (**12**)

Bond Distances

Zn1–O1	1.979(9)	Zn3–N91	2.04(1)	C1–O2	1.24(2)
Zn2–O1	2.618(9)	Zn4–N111	2.05(1)	Zn1–Zn2	4.595(3)
Zn1–N11	2.041(8)	C2–O4	1.28(1)	Zn3–O5	2.382(8)
Zn1–N31	2.04(1)	C2–O6	1.27(2)	Zn4–O6	1.913(9)
Zn2–N51	2.05(1)	Zn1–O2	2.335(8)	Zn3–N81	2.082(7)
C1–O1	1.28(1)	Zn2–O3	1.907(8)	Zn4–N101	2.01(1)
C1–O3	1.27(2)	Zn1–N21	2.068(7)	Zn4–N121	2.047(7)
Zn3–O4	1.957(9)	Zn2–N41	2.01(1)	C2–O5	1.24(2)
Zn4–O4	2.625(9)	Zn2–N61	2.022(8)	Zn3–Zn4	4.580(3)
Zn3–N71	2.033(9)				

Bond Angles

O1–Zn1–O2	58.8(3)	N81–Zn3–N91	89.9(3)	N51–Zn2–N61	91.1(4)
O1–Zn1–N21	102.4(4)	O4–Zn4–N101	98.5(4)	Zn1–O1–C1	100.3(8)
O2–Zn1–N11	102.8(3)	O4–Zn4–N121	92.4(3)	Zn1–O2–C1	84.5(6)
O2–Zn1–N31	100.6(3)	O6–Zn4–N111	115.0(4)	O4–Zn3–O5	58.8(3)
N11–Zn1–N31	94.5(4)	N101–Zn4–N111	89.9(4)	O4–Zn3–N81	103.8(3)
O1–Zn2–O3	32.0(2)	N111–Zn4–N121	91.4(4)	O5–Zn3–N71	102.5(3)
O1–Zn2–N51	168.9(3)	Zn3–O4–C2	101.3(8)	O5–Zn3–N91	100.3(3)
O3–Zn2–N41	125.3(3)	Zn3–O5–C2	82.6(6)	N71–Zn3–N91	92.8(3)
O3–Zn2–N61	128.1(4)	O1–Zn1–N11	131.9(3)	O4–Zn4–O6	26.0(2)
N41–Zn2–N61	97.5(4)	O1–Zn1–N31	130.6(3)	O4–Zn4–N111	170.1(3)
Zn1–O1–Zn2	176.1(3)	O2–Zn1–N21	161.1(4)	O6–Zn4–N101	125.1(4)
Zn2–O1–C1	76.2(7)	N11–Zn1–N21	91.8(3)	O6–Zn4–N121	126.6(4)
Zn2–O3–C1	109.6(6)	N21–Zn1–N31	90.0(3)	N101–Zn4–N121	98.6(3)
O4–Zn3–N71	131.6(3)	O1–Zn2–N41	97.9(4)	Zn3–O4–Zn4	176.5(4)
O4–Zn3–N91	132.1(3)	O1–Zn2–N61	94.8(3)	Zn4–O4–C2	75.6(7)
O5–Zn3–N81	162.3(4)	O3–Zn2–N51	113.7(4)	Zn4–O6–C2	108.9(7)
N71–Zn3–N81	91.4(3)	N41–Zn2–N51	90.6(4)		

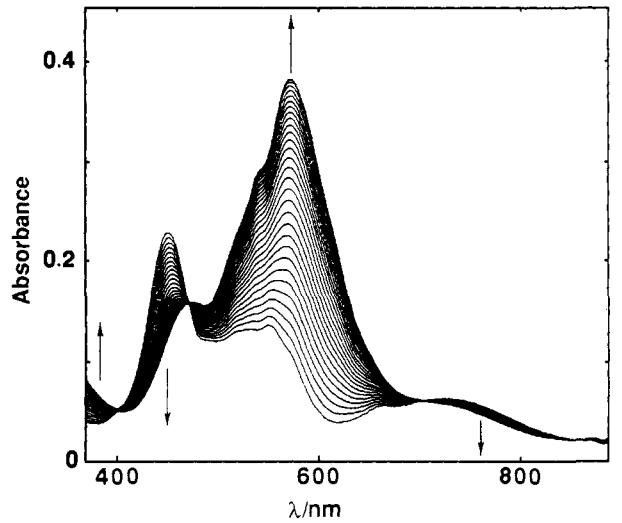

Figure 6. Time-dependent change of the electronic spectra during the reaction of $[Co(HB(3,5\text{-}iPr_2pz)_3)]_2(OH)_2$ (**3**) with atmospheric CO_2 in toluene (2.90 mM). Scans repeated with a cycle time of 90 min.

anhydrase forms a bidentately and tightly bound bicarbonate species which does not undergo further catalytic reaction effectively as discussed above. The other possibility is that Cu(II)-substituted carbonic anhydrase has a distinct coordination structure; not tetrahedral but tetragonal. This is quite likely when one considers the striking preference of Cu(II) ion to favor tetragonal coordination over tetrahedral, as seen in the crystal structures of **5** and **11**. Thus, there is no guarantee that Cu(II)-substituted carbonic anhydrase will form a tetrahedral hydroxo copper species as do other metal-substituted carbonic anhydrases. Rather, it is suggested that the copper-substituted carbonic anhydrase adopts a tetragonal coordination structure, most likely square-pyramidal. In fact, the copper-substituted carbonic anhydrase exhibits a d–d band at ca. 750 nm,[38] which is indicative of five-coordination geometry; from our series of studies, tetrahedral copper(II) complexes give rise to the d–d bands at ca. 900–1100 nm, while square-pyramidal complexes exhibit bands at ca. 700–800 nm.[39] Hence, the structure and reactivity of copper-substituted carbonic anhydrase may not be paralleled with those of other metal-substituted carbonic anhydrases. The structural factor, however, should be taken into account in comparing the activities of other metal-substituted carbonic anhydrases as well. Again there is no guarantee that the metal centers in substituted carbonic anhydrase adopt tetrahedral geometry as does the zinc center. Clearly, much structure/reactivity information from both the protein and the model studies is necessary to address the effect of the coordination environment of the metal site on the activity in carbonic anhydrase.

Experimental Section

Instrumentation. ^1H- and ^{13}C-NMR spectra were recorded on either a JEOL-GX-270 (270 MHz for ^1H, 67 MHz for ^{13}C) or JEOL-GX-500 (500 MHz for ^1H) spectrometer at 25 °C. The chemical shifts are reported as values (δ, ppm) downshifted from the internal standard Me_4Si. IR measurements were carried out in KBr using either a Hitachi 260-50 or a Nippon Bunko FT/IR-3 instrument. Electronic spectra and FD-MS spectra were recorded on a Shimazu UV-260 and a Hitachi M-80 spectrometer, respectively. The X-ray data collections were performed on either a Rigaku four-circle diffractometer (AFC-5) attached with a low-temperature apparatus or a Rigaku four-circle diffractometer (AFC-5R). Magnetic susceptibilities were determined by the Faraday method at 25 °C on a magnetometer (Shimazu MB-100) at Ochanomizu University. The X-ray data analyses were completed by TEXSAN computed with a MICRO-VAX-II. The programs were provided by Rigaku.

Materials and Methods. All solvents used were purified by literature methods[40] and treated under argon prior to use. The reagents of the highest grade commercially available were used without further puri-

(37) (a) Nakon, R.; Rechani, P. R.; Angelici, R. J. *J. Am. Chem. Soc.* **1974**, *96*, 2117. (b) Hay, R. W.; Basak, A. K.; Pujari, M. P.; Perotti, A. *J. Chem. Soc., Dalton Trans.* **1989**, 197. (c) Chin, J.; Jubian, V. J. *J. Chem. Soc., Chem. Commun.* **1989**, 839.

(38) (a) Haffner, P.; Coleman, J. E. *J. Biol. Chem.* **1975**, *250*, 996. (b) Bertini, I.; Canti, G.; Luchinat, C.; Scozzafava, A. *J. Chem. Soc., Dalton Trans.* **1978**, 1269.

(39) Kitajima, N.; Fujisawa, K.; Moro-oka, Y., unpublished observations.

(40) Perrin, D. D.; Armarego, W. L.; Perrin, D. R. *Purification of Laboratory Chemicals*, 2nd ed.; Pergamon: New York, 1980.

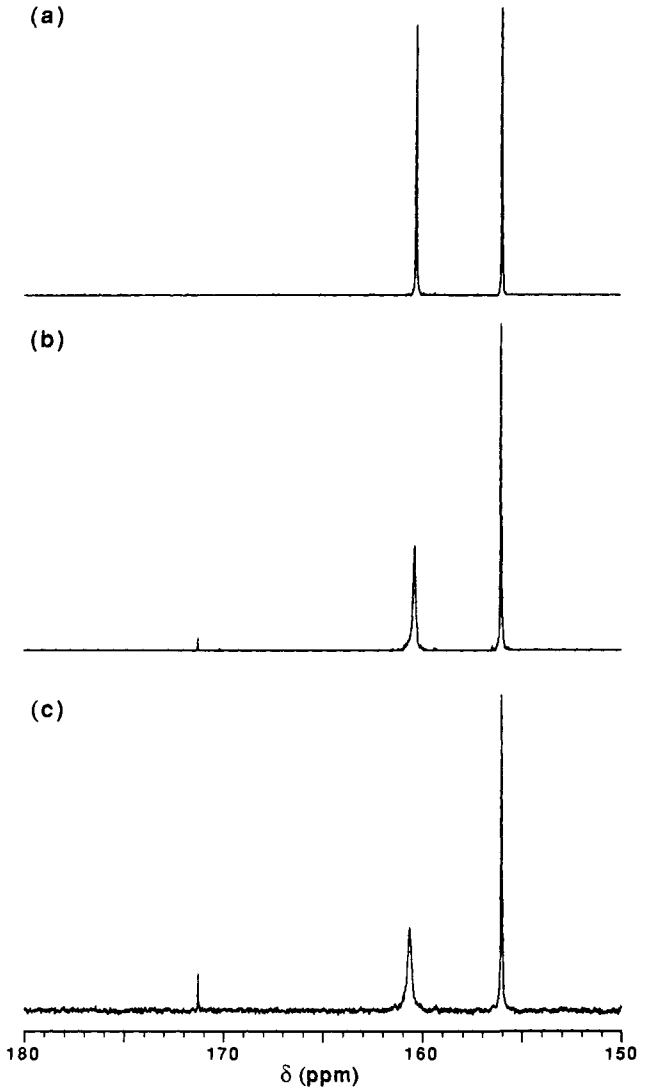

Figure 7. Reaction of $Zn(OH)(HB(3,5\text{-}iPr_2pz)_3)$ (**6**) with atmospheric CO_2 monitored by ^{13}C-NMR. (a) Spectrum of **6** in toluene-d_8 under argon (0.28 mM). (b) The atmosphere of the sample was replaced with air, and the NMR tube was sealed with a rubber cap. The spectrum was recorded after 5 days. (c) Spectrum of the sample from b recorded after 14 days.

fication. All preparations of the complexes were performed under argon by standard Schlenk techniques. $KHB(3,5\text{-}iPr_2pz)_3$ was prepared by the method described previously.[8b,21]

$Co(Cl)(HB(3,5\text{-}iPr_2pz)_3)$. $KHB(3,5\text{-}iPr_2pz)_3$ (1.388 g; 2.75 mmol) was stirred with 1 equiv of $CoCl_2$ (0.360 g; 2.77 mmol) in CH_2Cl_2 (40 mL) for 1 h. After filtration, the filtrate was dried under vacuum. The resulting solid was recrystallized from acetone (0.989 g; 1.77 mmol; 64%). Anal. Calcd for $C_{27}H_{46}N_6BClCo$: C, 57.92; H, 8.28; N, 15.01; Cl, 6.33. Found: C, 57.72; H, 8.62; N, 15.03; Cl, 6.35. ^1H-NMR (C_6D_6): δ −24 (3H), 0 (18H), 8 (18H), 13 (3H), 81 (3H). IR (cm^{-1}): 2547 (BH). UV–vis (toluene, nm, $\epsilon/M^{-1}\,cm^{-1}$): 633 (1300). FD-MS (*m/e*): 560.

$Co(NO_3)(HB(3,5\text{-}iPr_2pz)_3)$. In 60 mL of CH_2Cl_2 were stirred 3.130 g (6.20 mmol) of $KHB(3,5\text{-}iPr_2pz)_3$ and 1.917 g (6.59 mmol) of $Co(NO_3)_2{\cdot}6H_2O$ for 1 h. After removal of the salt by filtration, the filtrate was dried under vacuum. The resulting solid was recrystallized from MeCN, affording $Co(NO_3)(HB(3,5\text{-}iPr_2pz)_3)$ as red crystals (2.764 g; 4.71 mmol; 76% yield). Anal. Calcd for $C_{27}H_{46}N_7BO_3Co$: C, 55.30; H, 7.91; N, 16.72. Found: C, 54.81; H, 7.87; N, 16.85. ^1H-NMR (C_6D_6): δ −30 (3H), −12 (18H), 8 (18H), 24 (3H), 70 (3H). IR (cm^{-1}): 2556 (BH). UV–vis (toluene, nm, $\epsilon/M^{-1}\,cm^{-1}$): 571 (175), 722 (22). FD-MS (*m/e*): 587.

$[Co(HB(3,5\text{-}iPr_2pz)_3)]_2(OH)_2$ (3). In 25 mL of toluene was dissolved 0.516 g (0.88 mmol) of $Co(NO_3)(HB(3,5\text{-}iPr_2pz)_3)$. The solution was treated with 15 mL of 1 N aqueous NaOH for 30 min. The separated toluene phase was dried under vacuum. The resulting solid was recrystallized from pentane at −20 °C, yielding **3** as red crystals (0.296 g; 0.273 mmol; 62%). Anal. Calcd for $C_{54}H_{94}N_{12}B_2O_2Co_2$: C, 59.89; H, 8.75; N, 15.52. Found: C, 59.43; H, 8.53; N, 15.55. ^1H-NMR (toluene-d_8): δ −144 (6H), −57 (36H), 34 (36H), 51 (6H), 82 (6H). IR (cm^{-1}): 3700 (OH), 2541 (BH). UV–vis (toluene, nm, $\epsilon/M^{-1}\,cm^{-1}$): 453 (70), 551 (40), 730 (18). FD-MS (*m/e*): 1108 (main), 1064. μ_{eff}: 6.23 μ_B/mol.

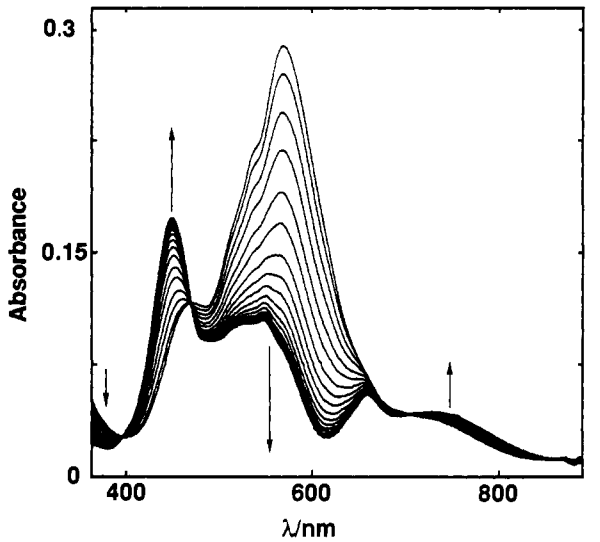

Figure 8. Time-dependent change of the electronic spectra during the reaction of $[Co(HB(3,5\text{-}iPr_2pz)_3)]_2(CO_3)$ (**9**) with aqueous 1 N NaOH solution under argon. The toluene solution of **9** (4 mL, 2.37 mmol) was layered onto 0.2 mL of aqueous NaOH in a quartz cell (1-cm length), and the spectra were recorded with a cycle time of 30 min. The final spectrum is in good accord with that of the hydroxo complex **3** (see Figure 6).

$Ni(Cl)(HB(3,5\text{-}iPr_2pz)_3)$. A THF solution of $KHB(3,5\text{-}iPr_2pz)_3$ (1.819 g; 3.60 mmol; in 50 mL) was mixed with a MeOH solution of $NiCl_2{\cdot}6H_2O$ (0.876 g; 3.69 mmol; in 20 mL) and stirred for 20 min. After removal of the solvent under vacuum, the resulting solid was dissolved in CH_2Cl_2 and the solution was filtered to eliminate the salt. The filtrate was dried under vacuum to afford pink-colored powder which was washed with pentane and MeCN (1.509 g; 2.70 mmol; 75% yield). Anal. Calcd for $C_{27}H_{45}N_6BClNi$: C, 57.95; H, 8.28; N, 15.02; Cl, 6.33. Found: C, 58.02; H, 8.39; N, 14.94; Cl, 5.95. ^1H-NMR (C_6D_6): δ −13 (1H), 1 (18H), 3 (18H), 4 (3H), 84 (3H). IR (cm^{-1}): 2518 (BH). UV–vis (toluene, nm, $\epsilon/M^{-1}\,cm^{-1}$): 481 (410), 801 (110). FD-MS (*m/e*): 560.

$[Ni(HB(3,5\text{-}iPr_2pz)_3)]_2(OH)_2$ (4). $Ni(Cl)(HB(3,5\text{-}iPr_2pz)_3)$ (0.307 g; 0.59 mmol) was dissolved in 15 mL of toluene. To the solution added was 1 N aqueous NaOH (10 mL), and the mixture was stirred for 30 min. The toluene phase was separated and dried under vacuum. Recrystallization of the resulting solid from pentane at −20 °C afforded **4** as yellowish green crystals (0.169 g; 0.156 mmol; 57% yield). Anal. Calcd for $C_{54}H_{94}N_{12}B_2O_2Ni_2$: C, 59.92; H, 8.75; N, 15.53. Found: C, 59.81; H, 8.60; N, 15.18. ^1H-NMR (C_6D_6): δ −8 (2H), 1 (36H), 2 (36H), 41 (6H). IR (cm^{-1}): 3670 (OH), 2538 (BH). UV–vis (toluene, nm, $\epsilon/M^{-1}\,cm^{-1}$): 400 (230), 477 (30), 667 (33). FD-MS (*m/e*): 1106 (main), 1062. μ_{eff}: 3.54 μ_B/mol.

$[Mn(HB(3,5\text{-}iPr_2pz)_3)]_2(OH)_2$ (1), $[Fe(HB(3,5\text{-}iPr_2pz)_3)]_2(OH)_2$ (2), and $[Cu(HB(3,5\text{-}iPr_2pz)_3)]_2(OH)_2$ (5). These complexes were synthesized by the methods reported previously.[8,19,20] The details of preparations of **1** and **2** will be described elsewhere.

$Zn(Br)(HB(3,5\text{-}iPr_2pz)_3)$. $KHB(3,5\text{-}iPr_2pz)_3$ (0.452 g; 0.90 mmol) and $ZnBr_2$ (0.219 g; 0.97 mmol) were stirred in a mixture of 20 mL of acetone and 40 mL of CH_2Cl_2 for 30 min. The formed precipitates were removed by filtration, and the concentrated filtrate was cooled overnight at −20 °C, affording the complex as colorless crystals (0.326 g; 0.53 mmol; 60% yield). Anal. Calcd for $C_{27}H_{46}N_6BBrZn$: C, 53.09; H, 7.59; N, 13.76; Br, 13.08. Found: C, 53.31; H, 7.38; N, 13.84; Br, 13.42. ^1H-NMR (C_6D_6): δ 1.11 (d, J = 7.0 Hz, 18H, $CHMe_2$), 1.23 (d, J = 7.0 Hz, 18H, $CHMe_2$), 3.48 (m, J = 7.0 Hz, 3H, $CHMe_2$), 3.83 (m, J = 7.0 Hz, 3H, $CHMe_2$), 5.81 (s, 3H, pz). ^{13}C-NMR (C_6D_6): δ 23.4 ($CHMe_2$), 23.5 ($CHMe_2$), 26.5 ($CHMe_2$), 27.5 ($CHMe_2$), 98.1 (pz-C—H), 156.4 (pz-C=N), 161.3 (pz-C=N). IR (cm^{-1}): 2539 (BH). FD-MS (*m/e*): 611.

Table IV. Crystal Data and Data Collection Details of **3**·2C_5H_{12}, **4**·2C_5H_{12}, **8**·2MeCN, **9**·2MeCN, **10**·Me_2CO, **11**·2MeCN, and **12**

	3·2C_5H_{12}	**4**·2C_5H_{12}	**8**·2MeCN	**9**·2MeCN	**10**·Me_2CO	**11**·2MeCN	**12**
formula	$C_{64}H_{118}N_{12}O_2B_2Co_2$	$C_{64}H_{118}N_{12}O_2B_2Ni_2$	$C_{59}H_{98}N_{14}O_3B_2Fe_2$	$C_{59}H_{98}N_{14}O_3B_2Co_2$	$C_{58}H_{98}N_{12}O_4B_2Ni_2$	$C_{59}H_{98}N_{14}O_3B_2Cu_2$	$C_{55}H_{92}N_{12}O_3B_2Zn_2$
formula weight	1227.21	1226.72	1184.84	1162.99	1166.50	1200.23	1121.82
crystal system	triclinic	triclinic	triclinic	triclinic	monoclinic	orthorhombic	triclinic
space group	$P\bar{1}$	$P\bar{1}$	$P\bar{1}$	$P\bar{1}$	$P2_1/a$	$Pbca$	$P\bar{1}$
a/Å	14.563(3)	14.531(8)	14.252(3)	14.181(3)	26.905(9)	24.058(7)	26.807(9)
b/Å	22.493(5)	22.460(5)	25.892(4)	25.718(6)	12.813(5)	25.664(5)	27.711(14)
c/Å	14.033(4)	14.017(7)	9.617(3)	9.647(3)	19.401(5)	22.844(6)	9.877(2)
α/deg	93.10(2)	93.07(3)	90.25(2)	90.13(3)	90.0	90.0	97.87(3)
β/deg	126.05(1)	125.95(3)	97.34(2)	96.92(3)	98.87(3)	90.0	91.16(3)
γ/deg	97.92(2)	98.12(3)	107.15(1)	106.74(2)	90.0	90.0	66.52(3)
V/Å^3	3628(2)	3613(3)	3360(1)	3342(2)	6608(7)	14104(6)	6661(3)
Z	2	2	2	2	4	8	4
d(calcd)/g cm^{-3}	1.12	1.13	1.17	1.16	1.17	1.13	1.12
crystal size/mm^3	0.7 × 0.5 × 0.4	0.4 × 0.3 × 0.3	0.4 × 0.2 × 0.3	0.4 × 0.2 × 0.15	0.2 × 0.2 × 0.1	0.2 × 0.2 × 0.3	0.3 × 0.2 × 0.15
data collection t/°C	−50	−50	−60	−50	23	23	23
radiation	graphite-monochromatized Mo Kα (λ = 0.710 68 Å)						
μ(Mo Kα)/cm^{-1}	5.00	5.68	4.79	5.43	6.16	6.48	7.81
scan mode	$\omega - 2\theta$	$\omega - 2\theta$	$\omega - 2\theta$	$\omega - 2\theta$	ω	ω	ω
scan width/deg	1.30 + 0.14 tan θ	1.30 + 0.14 tan θ	1.30 + 0.14 tan θ	1.30 + 0.14 tan θ	1.05 + 0.14 tan θ	0.97 + 0.14 tan θ	1.09 + 0.14 tan θ
scan speed/deg·min^{-1}	6	6	6	6	8	8	16
2θ range	2–50°	2–50°	3–50°	3–50°	2–50°	5–50°	5–45°
octant measure	$\pm h,\pm k,+l$	$\pm h,\pm k,+l$	$\pm h,\pm k,+l$	$\pm h,\pm k,+l$	$+h,+k,\pm l$	$+h,+k,+l$	$+h,\pm k,\pm 1$
no. of measured reflections	11 310	11 315	9529	10 767	8450	7350	17 845
no. of observed reflections	9547	9605	6719	8944	8145	5749	10 250
	($F_o \geq 3\sigma F_o$)	($F_o \geq 3\sigma F_o$)	($F_o \geq 3\sigma F_o$)	($F_o \geq 3\sigma F_o$)	($F_o \geq 3\sigma F_o$)	($F_o \geq 6\sigma F_o$)	($F_o \geq 3\sigma F_o$)
R/%	7.20	9.66	7.34	6.72	3.94	5.06	8.23
R_w/%	6.76	8.44	6.39	5.16	5.20	7.08	11.02

Zn(OAc)(HB(3,5-iPr$_2$pz)$_3$). A mixture of 1.032 g (2.04 mmol) of KHB(3,5-iPr$_2$pz)$_3$ and 0.503 g (2.29 mmol) of Zn(OAc)$_2$ 2H$_2$O was stirred in 30 mL of CH_2Cl_2 for 1 h. After removal of the salt by filtration, the solution was dried under vacuum. Recrystallization of the resulting solid from MeCN at −20 °C gave Zn(OAc)(HB(3,5-iPr$_2$pz)$_3$) as colorless crystals (0.977 g; 1.66 mmol; 81% yield). Anal. Calcd for $C_{29}H_{49}N_6BO_2Zn$: C, 59.04; H, 8.37; N, 14.24. Found: C, 58.94; H, 8.32; N, 14.59. ^{1}H-NMR ($CDCl_3$): δ 1.14 (d, J = 7.4 Hz, 18H, CHMe_2), 1.25 (d, J = 7.4 Hz, 18H, CHMe_2), 2.35 (s, 3H, OOCMe), 3.54 (m, J = 7.3 Hz, 3H, CHMe$_2$), 3.70 (m, J = 7.3 Hz, 3H, CHMe$_2$), 5.83 (s, 3H, pz). ^{13}C-NMR ($CDCl_3$): δ 21.9 (OOCMe), 23.1 (CHMe_2), 23.4 (CHMe_2), 26.1 (CHMe$_2$), 26.8 (CHMe$_2$), 97.3 (pz-C—H), 155.8 (pz-C=N), 159.9 (pz-C=N), 179.4 (OOCMe). IR (cm^{-1}): 2549 (BH), 1601 (C=O), 1331 (C=O). FD-MS (m/e): 589.

Zn(OH)(HB(3,5-iPr$_2$pz)$_3$) (6). An Et$_2$O solution of Zn(OAc)(HB(3,5-iPr$_2$pz)$_3$) (0.547 g; 0.93 mmol; in 20 mL) was stirred with 10 mL of 0.1 N aqueous NaOH for 15 min. The Et$_2$O phase was separated and dried under vacuum to give an analytically pure sample of **6** as a white solid in 90% yield. Owing to its extremely high solubility in any solvent we tried, recrystallization was not completed. Anal. Calcd for $C_{27}H_{47}N_6BOZn$: C, 59.19; H, 8.65; N, 15.34. Found: C, 59.57; H, 9.01; N, 15.00. ^{1}H-NMR (C_6D_6): δ 1.13 (d, J = 6.1 Hz, 18H, CHMe_2), 1.26 (d, J = 6.1 Hz, 18H, CHMe_2), 3.48 (m, J = 6.1 Hz, 3H, CHMe_2), 3.50 (m, J = 6.1 Hz, 3H, CHMe$_2$), 5.81 (s, 3H, pz). No proton signal attributable to the OH was observed as reported for Zn(OH)(HB(3-Me-5-tBupz)$_3$).[6] ^{13}C-NMR ($CDCl_3$): δ 23.1 (CHMe_2), 23.3 (CHMe_2), 26.0 (CHMe$_2$), 27.2 (CHMe$_2$), 97.0 (pz-C—H), 155.9 (pz-C=N), 159.5 (pz-C=N). IR (cm^{-1}): 3670 (OH), 2547 (BH). FD-MS (m/e): 1122 (100%, due to LZn(CO$_3$)ZnL), 530 (30%).

Preparations of the μ-Carbonato Dinuclear Complexes 7–12. Under argon, the hydroxo complex was dissolved in toluene in a Schlenk tube. The atmosphere in the Schlenk was replaced with pure CO_2 with cooling the solution at −78 °C. The solution was warmed to room temperature and stirred for 1 h. After removal of toluene, the resulting solid was recrystallized, affording the carbonato complex as a microcrystalline solid.

[Mn(HB(3,5-iPr$_2$pz)$_3$)]$_2$(CO$_3$) (7). Recrystallization from MeCN gave **7** as colorless crystals in 64% yield. Anal. Calcd for $C_{55}H_{92}N_{12}B_2O_3Mn_2$: C, 60.01; H, 8.42; N, 15.27. Found: C, 59.54; H, 8.49; N, 15.11. IR (cm^{-1}): 2545 (BH), 1650–1550 (sh, C=O). FD-MS (m/e): 1101. μ_{eff}: 7.53 μ_B/mol.

[Fe(HB(3,5-iPr$_2$pz)$_3$)]$_2$(CO$_3$) (8). Recrystallization from MeCN gave **8** as colorless crystals in 42% yield. Anal. Calcd for $C_{55}H_{92}N_{12}B_2O_3Fe_2$: C, 59.91; H, 8.41; N, 15.24. Found: C, 60.20; H, 8.69; N, 15.54. ^{1}H-NMR (toluene-d_8): δ −5 (36H), 6 (36H), 17 (6H), 57 (6H). IR (cm^{-1}): 2523 (BH), 1650–1530 (sh, C=O). FD-MS (m/e): 1103. μ_{eff}: 6.96 μ_B/mol. The single crystals for the X-ray study were obtained from **8** prepared as follows: a toluene solution of Fe(Cl)(HB(3,5-iPr$_2$pz)$_3$) (0.228 g; 0.41 mmol; in 30 mL) was treated with aqueous NaHCO$_3$ (0.100 g; in 10 mL) under argon carefully (0.133 g; 0.12 mmol; 59% yield).

[Co(HB(3,5-iPr$_2$pz)$_3$)]$_2$(CO$_3$) (9). Recrystallization from MeCN gave **9** as blue purple crystals in 78% yield. Anal. Calcd for $C_{55}H_{92}N_{12}B_2O_3Co_2$: C, 59.57; H, 8.36; N, 15.16. Found: C, 59.15; H, 8.61; N, 15.14. ^{1}H-NMR (toluene-d_8): δ −70 (6H), −26 (36H), 14 (36H), 41 (6H), 45 (6H), 77 (2H). IR (cm^{-1}): 2541 (BH), 1650–1560 (sh, C=O). UV-vis (toluene, nm, ϵ/M^{-1} cm^{-1}): 480 (sh), 572 (112), 720 (sh). FD-MS (m/e): 1108. μ_{eff}: 5.84 μ_B/mol.

[Ni(HB(3,5-iPr$_2$pz)$_3$)]$_2$(CO$_3$) (10). Recrystallization from MeCN gave **10** as green crystals in 82% yield. Anal. Calcd for $C_{55}H_{92}N_{12}B_2O_3Ni_2$: C, 59.60; H, 8.37; N, 15.16. Found: C, 59.64; H, 8.52; N, 15.60. ^{1}H-NMR (C_6D_6): δ −3 (2H), 0 (36H), 2 (36H), 3 (6H), 40 (6H). IR (cm^{-1}): 2540 (BH), 1581 (C=O). UV-vis (toluene, nm, ϵ/M^{-1} cm^{-1}): 408 (409), 665 (73), 848 (55). FD-MS (m/e): 1106. μ_{eff}: 3.25 μ_B/mol.

[Cu(HB(3,5-iPr$_2$pz)$_3$)]$_2$(CO$_3$) (11). Recrystallization from MeCN gave **11** as green crystals in 65% yield. Anal. Calcd for $C_{55}H_{92}N_{12}B_2O_3Cu_2$: C, 59.08; H, 8.29; N, 15.03. Found: C, 58.82; H, 8.01; N, 15.40. ^{1}H-NMR (C_6D_6): δ 1.16 (d, J = 6.6 Hz, 18H, CHMe_2), 1.64 (s, br, 18H, CHMe_2), 3.55 (m, J = 6.6 Hz, 3H, CHMe$_2$), 3.76 (s, br, 3H, CHMe$_2$), 6.07 (s, br, 3H, pz). IR (cm^{-1}): 2533 (BH), 1593 (C=O). UV-vis (CH_2Cl_2, nm, ϵ/M^{-1} cm^{-1}): 349 (12 400), 670 (440). FD-MS (m/e): 1118. μ_{eff}: 0.53 μ_B/mol.

[Zn(HB(3,5-iPr$_2$pz)$_3$)]$_2$(CO$_3$) (12). Recrystallization from pentane gave **12** as colorless crystals in 68% yield. Anal. Calcd for $C_{55}H_{92}N_{12}B_2O_3Zn_2$: C, 58.89; H, 8.27; N, 14.98. Found: C, 59.04; H, 8.62; N, 14.66. ^{1}H-NMR ($CDCl_3$): δ 1.09 (d, J = 7.3 Hz, 36H, CHMe_2), 1.23 (d, J = 7.3 Hz, 36H, CHMe_2), 3.33 (m, J = 7.3 Hz, 6H, CHMe$_2$), 3.46 (m, J = 7.3 Hz, 6H, CHMe$_2$), 5.88 (s, 6H, pz). ^{13}C-NMR (toluene-

d_8): δ 23.5 (CHMe_2), 23.8 (CHMe_2), 26.6 (CHMe_2), 27.5 (CHMe_2), 97.5 (pz-C—H), 155.9 (pz-C—H), 160.9 (pz-C=N), 171.3 (CO_3). IR (cm^{-1}): 2547 (BH), 1700–1520 (br-sh, C=O). FD-MS (m/e): 1122.

Evaluation of CO_2 Fixation Rates of the Hydroxo Complexes. Comparison of the rates of Co (**3**), Ni (**4**), and Cu (**5**) hydroxo complexes for CO_2 fixation was accomplished by electronic spectroscopy. In a 50-mL Schlenk tube, 1.0 mL of a toluene solution (15 mM) of the complex was injected by a syringe through a septum cap under 1 atm of Ar. CO_2 (1 atm, 1 mL) was then introduced into the tube by a gas-tight syringe. The solution was allowed to stand for a prescribed time at room temperature without stirring, and the visible spectrum was recorded under argon. The conversions to the μ-carbonato complex were determined as follows for the reaction times: 2.5 min, **3**, 20%; **4**, 35%; **5**, 40%; 5 min, **3**, 42%; **4**, 50%; **5**, 59%; 10 min, **3**, 63%; **4**, 76%; **5**, 81%. The reproducibility of the experiments was checked, indicating the experimental error within 3%. Thus the order of activity of these three complexes was concluded to be Cu > Ni > Co. The rate of Zn complex **6** was determined by ^{1}H-NMR. A solution of **6** (32 mM in C_6D_6) was prepared under argon. A portion of the solution (1.0 mL) was transferred into a 50-mL Schlenk tube under 1 atm of Ar, and 0.5 mL of CO_2 (1 atm) was injected by a gas-tight syringe through a septum cap. After being allowed to stand without stirring for a prescribed reaction time, the solution was transferred into a NMR tube and its ^{1}H-NMR spectrum was recorded by a 500-MHz NMR instrument. The conversion of **6** to the μ-carbonato complex **12** was determined from the integrated areas of the signals at 5.81 and 5.88 ppm attributable to the pyrazole-4-protons of **6** and **12**, respectively. The same experiments were performed for Ni (**4**) and Cu (**5**) complexes under the exact same conditions. The determined conversions are as follows for the reaction times: 5 min, **4**, 36%; **5**, 44%; **6**, 51%; 10 min, **4**, 46%; **5**, 58%; **6**, 72%. The experimental errors are within 5%. Thus it is evident the Zn complex **6** is more effective for CO_2 fixation than **4** and **5**. The relative rate of CO_2 fixation of the Mn complex **1** to that of Co (**4**) was determined by FT-IR with monitoring the decrease of the ν(OH) band, indicating that **4** is more effective than **1**. The evaluation of the reactivity of Fe complex **2** was very difficult owing to its extremely air-sensitivity. But the fact that the complete conversion of **2** to the carbonato complex **8** took more than 10 min (from ^{1}H-NMR) under 1 atm of pure CO_2 led us to conclude that **2** is the most inert hydroxo complex, because the conversions of other hydroxo complexes take place completely within a few minutes under the same reaction conditions. Consequently, the order of reactivities determined is Zn (**6**) > Cu (**5**) > Ni (**4**) ≈ Co (**3**) > Mn (**1**) > Fe (**2**).

X-ray Data Collections and Structural Determinations. Single crystals of **3**·2C_5H_{12} and **4**·2C_5H_{12} were obtained by recrystallization from pentane at −20 °C. In order to avoid the loss of the pentane of crystallization, the data collections were completed at −50 °C with sealing the crystal in a thin-wall glass capillary. Crystals suitable for X-ray diffractions of **8**·2MeCN, **9**·2MeCN, and **11**·MeCN were obtained by slow evaporation of the MeCN solutions. The data of **8**·2MeCN and **9**·2MeCN were recorded at −60 °C and −50 °C, respectively. Since the crystal **11**·2MeCN was reasonably stable when it was sealed in a glass capillary, the data were collected at 23 °C. Crystals of **10**·Me_2CO and **12** were obtained by recrystallization from acetone/MeOH and MeOH, respectively, and the data collections were performed at 23 °C. A Mo X-ray source equipped with a graphite monochromator (Mo Kα, λ = 0.710 680 Å) was used. Automatic centering and least-squares routines were carried out for all the compounds with 25 reflections of 20° < 2θ < 30° to determine the cell parameters. Data collections were completed with ω − 2θ or ω scan. All data were corrected for Lorentz and polarization effects but not absorption. Intensities of three checked reflections monitored every 100 reflections showed no serious decay. A summary of cell parameters, data collection conditions, and refinement results for **3**·2C_5H_{12}, **4**·2C_5H_{12}, **8**·2MeCN, **9**·2MeCN, **10**·Me_2CO, **11**·2MeCN, and **12** is provided in Table IV.

The initial positional parameters of the metal atoms in **3**·2C_5H_{12}, **4**·2C_5H_{12}, and **12** were determined by the Patterson method. The structures of the other complexes were determined by the direct method: for **8**·2MeCN, SAPI85, and for **9**·2MeCN, **10**·Me_2CO, and **11**·2MeCN, MITHRIL. Subsequent difference Fourier syntheses easily located all non-hydrogen atoms. All non-hydrogen atoms except solvents of crystallization were refined anisotropically by TEXSAN. The hydrogen atoms except on the solvent of crystallization were calculated and isotropically fixed in the final refinement cycles except **12** (d(C-H) = 1.0 Å, with the isotropic thermal factor of U_{iso}(H) = 1.2U_{iso}(C)). The final R and R_w factors are given in Table IV, where $R = \sum(|F_o| - |F_c|)/\sum|F_o|$ and $R_w = \sum[w(|F_o| - |F_c|)^2/\sum w|F_o|^2]^{1/2}$ with $w = 1/\sigma^2(F_o^2)$.

Full bond lengths, bond angles, and anisotropic temperature factors for non-hydrogen atoms, hydrogen coordinates, and F_o/F_c tables for **3**·2C_5H_{12}, **4**·2C_5H_{12}, **8**·2MeCN, **9**·2MeCN, **10**·Me_2CO, **11**·2MeCN, and **12** are available as supplementary material.

Acknowledgment. We thank Prof. Y. Fukuda of Ochanomizu University for kind help in measuring the magnetic susceptibilities and Prof. G. Parkin of Columbia University for the precopy of ref 26 and stimulating discussions. This research was supported in part from a Grant-in-Aid for Scientific Research from the Japanese Ministry of Education, Culture, and Science (03241106 and 03750598), to which we are grateful.

Supplementary Material Available: Tables of crystal data, atomic coordinates and temperature factors, hydrogen coordinates, and intramolecular bond distances and angles (106 pages); tables of observed and calculated structure factors for **3**·2C_5H_{12}, **4**·2C_5H_{12}, **8**·2MeCN, **9**·2MeCN, **10**·Me_2CO, **11**·2MeCN, and **12** (203 pages). Ordering information is given on any current masthead page.